

Effect of density changes on tokamak plasma confinement

F. Spineanu^{1, a)} and M. Vlad¹

*National Institute of Laser, Plasma and Radiation Physics Bucharest,
Romania*

(Dated: January 27, 2022)

A change of the particle density (by gas puff, pellets or impurity seeding) during the plasma discharge in tokamak produces a radial current and implicitly a torque and rotation that can modify the state of confinement. After ionization the newly born ions will evolve toward the periodic neoclassical orbits (trapped or circulating) but the first part of their excursion, which precedes the periodicity, is an effective radial current. It is short, spatially finite and unique for each new ion, but multiplied by the rate of ionization and it can produce a substantial total radial current. The associated torque induces rotation which modify the transport processes. We derive the magnitude of the radial current induced by ionization by three methods: the analysis of a simple physical picture, a numerical model and the neoclassical drift-kinetic treatment. The results of the three approaches are in agreement and show that the current can indeed be substantial. Many well known experimental observations can be reconsidered under this perspective. In reactor-grade plasma the confinement can be strongly influenced by adequate particle fuelling.

PACS numbers: 52.55.Fa, 52.20.Dq, 52.25.Fi

^{a)}florin.spineanu@euratom.ro

I. INTRODUCTION

Every event of ionization of a neutral particle in tokamak plasma is followed by the displacement of the newly born charges (electron and ion) towards the equilibrium orbits. They leave the magnetic surface where they have been created, due to the neoclassical drift, and evolve towards stationary trajectories. Since the electrons drift much less than the ions, the main effect is associated with the newly born ions. Neglecting collisions, the ions will settle on circulating or trapped orbits and during the periodic motions they depart radially, relative to a certain magnetic surface, alternatively to larger and respectively to smaller radius. Since these positive and negative radial deviations relative to the magnetic surface compensate, the time average shows no effective radial displacement: the orbit has an effective “center” which corresponds to the spatial average of the successive positions of the ion (for example: the “center” of a banana, for the trapped ion; we neglect smaller neoclassical motions of this “center”, like the toroidal drift). However there is a part in the radial excursion of the new ion which remains uncompensated. This is precisely the first interval, just after the ionization, when the ion evolves to take the periodic trajectory, and its successive positions do not yet average to the “center”. This displacement, from the position where ionization takes place, towards the “center” of the periodic trajectory, is an effective radial current. At the end of this finite, transitory part, the motion becomes periodic and there is no radial current. The radial current of the first part is a source of torque, implicitly rotation and in this way has an impact on the quality of the confinement. It effectively makes a connection between the density change (via pellets, gas puff or impurity seeding) and the change of the confinement. We note that there is a considerable experimental evidence that the variation of density (during the discharge) produces a change in the quality of the confinement.

On a fast time scale a radial electric field is generated by the charge separation: the electrons are almost tied to the magnetic surface, while the ions will travel with the neoclassical drift velocity to their “center”, on a distance about half of a banana width. We estimate the radial current and obtain an order of magnitude of the rate of the torque. Compared with the damping rate of a poloidal rotation by transit time magnetic pumping, the ionization-induced rate can be substantially higher. Some improved regimes in JET, as “pellet enhanced performance” (PEP)^{24, 14}, DIII-D^{15, 1} and confinement changes observed

in many devices^{6, 30, 17, 29} appear to be connected with this effect of density variation.

The ionization-induced torque has a direction which is fixed by neoclassical orbit's geometry and it interacts with any pre-existing rotation which may have been induced by Reynolds stress, Stringer mechanism or by external factors (NBI, ICRH). The new torque can enhance the pre-existing rotation or can act against it, which makes difficult to predict its consequences in all situations.

We suggest that this process may be a unifying connection between a wide class of regimes where it has been noted a correlation between a dynamic change of density (within a discharge) and the change of the confinement.

According to the preceding explanation, there are two mechanisms that are responsible for this connection

(1) the change of density via ionization (of a pellet, gas puff, impurity seeding or influx of neutral atoms from the edge) means that $\sqrt{\varepsilon}$ ($\varepsilon = r/R$) fraction of the newly created ions are trapped and are moving radially to occupy the positions (the “centers”) which are the averages of positions on the trapped (banana) orbits. While after arriving there the bounce averaged radial displacement is zero for the trapped ion, the first step, when the ion moves from the place where it has been created to the “center” of the banana is a net radial current, a single and unrepeatable event for every ionization event. The ensemble of such events is a radial current that produces a torque which generates poloidal rotation and sustains it against magnetic pumping²⁷; the sheared poloidal rotation is a barrier that reduce the turbulence and enhances the confinement.

(2) every conversion of a trapped ion into a circulating one (and equally the reversed process), is accompanied by a substantial radial drift. This is because the “centers” of the two kinds of orbits are different and the change from one type of periodic motion (*e.g.* trapped) to the other type of periodic motion (circulating) goes through an intermediate regime, unique and transitory. It consists of the last part of the motion on banana, when the periodicity is lost, followed by the first part of the motion, until the new periodicity is established. Both these parts are unique and transitory and are manifested as a radial current which produces a torque. Then any dynamic process which implies a (slow or fast) change in the velocity space in the region: trapped/circulating ions, will produce a torque. It is interesting to note that this is a mechanism of *direct* coupling between the toroidal and

poloidal rotation. If for some reason a toroidal flow occurs in plasma, a number of trapped ions will have increased their parallel velocity and will change from trapped to circulating¹⁹. The associated radial current produces a poloidal torque. Conversely, stopping the toroidal rotation leads a subset of the ion population to convert from circulating to trapped, which again produces a transient radial current and further poloidal rotation.

In the present work we concentrate on only the first of the two processes.

Several effects can be connected with this ionization-induced torque. Regimes that are confirmed by experiments, like the mentioned PEP, density peaking and/or anomalous density pinch may have a connection with this torque. The dynamic charge separation that occurs when the ions move from the place of ionization to the “center” of the neoclassical periodic orbit induces a return current of the background ions. Since the number of new ions generated by ionization of a pellet is episodically comparable with the local background ion density, the response motion of this latter population takes the aspect of a massive, even if short, radial displacement. On a relatively large space interval, on which the radial derivative of the rate of ionization [$\partial S/\partial x$ in Eq.(22) below] keeps the same sign, the displacement of the background ions has a unique direction and is sustained all along the total time of ionization. This appears as a density pinch, eventually contributing to the density peaking. Since this equally involves the impurity ions, it can provide a new mechanism for the impurity accumulation.

We note that the ionization of impurity atoms leads to much larger radial drifts and in consequence larger radial currents and torque. This must be examined in relation with impurity (argon) seeding at the edge and with *Li* pellets in the core. In general any influx of neutral atoms in the plasma will be a source of rotation which affects the local conditions, including the possibility of being a trigger for the *L* to *H* mode transition.

We give in the next Sections a simple description of the statistical build-up of a radial current associated with the ionization. At this level of description the collisions are neglected, as are the dispersions of the absolute magnitude of velocities, and of the parallel velocities. The intention is to draw attention to the high amplitude of this current. Further, our result is confirmed by the drift-kinetic neoclassical approach, developed in parallel to the classical treatments of Rosenbluth and Hinton for the similar cases of the torque induced by *alpha* particles²³ and by *neutral beam injection* (NBI)¹².

II. ESTIMATION OF THE RADIAL CURRENT GENERATED AT IONIZATION

A. The contributions to the current

For an easier discussion we adopt a simple picture, mainly having in mind the pellet injection. The source is considered to be limited to a finite segment $[r_1, r_2]$ on the radius r , placed somewhere between $r = 0$ (magnetic axis) and $r = a$ (edge). Due to the symmetry we take the segment as lying in the equatorial plane. The words “left” or “right” refer to this segment, with left being closer to the magnetic axis. The newly born ions will move to place themselves on the periodic neoclassical trajectories, banana or circulating. A radial current is produced during only the first, unique and transitory, part of the trajectory, which is about half of the width of the banana.

We start with a purely geometric example. Consider the motion of a point on a circle C with radius R and center at $(x = R, y = 0)$ on the Ox axis. We introduce the angle $\theta(t)$ between the Ox axis and the radius from the center of the circle $(R, 0)$ to the position of the point on the circle (x, y) . θ increases clockwise. The point starts from the origin $(x = 0, y = 0)$, $\theta(t = 0) = 0$. The equations are: $x(t) = R - R \cos[\theta(t)]$ and $y(t) = R \sin[\theta(t)]$. The motion on C is assumed uniform $\theta(t) = \omega t$. The average of the positions of the point $(x(t), y(t))$ up to the current time t are $\bar{x}(t) = \frac{1}{t} \int_0^t dt' x(t') = R - \frac{1}{t} R \frac{1}{\omega} \sin(\omega t)$ with $\bar{x}(t = 0) = 0$ and $\bar{y}(t) = \frac{1}{t} \int_0^t dt' R \sin(\omega t') = \frac{R}{\omega t} [1 - \cos(\omega t)]$, with $\bar{y}(t = 0) = 0$. Clearly the asymptotic $t \rightarrow \infty$ average position will be $(R, 0)$, which is the “center” and, after a transient phase, the motion is periodic. The speed with which the average position moves is $d\bar{x}/dt = (R/\omega) t^{-2} \sin(\omega t) - R t^{-1} \cos(\omega t)$. We note that the y -projection of the average, $\bar{y}(t)$, is always positive and that for small time, $t \ll \omega^{-1}$, the x -projected average is linear in time $\bar{x}(t) \approx (R\omega^2/3)t$. Both properties will also be found for banana orbits.

The speed of the ions on this transient part of its motion is the neoclassical drift velocity $\mathbf{v}_{Di} = (1/\Omega_{ci}) \hat{\mathbf{n}} \times (\mu \nabla B + v_{\parallel}^2 (\hat{\mathbf{n}} \cdot \nabla) \hat{\mathbf{n}}) \approx \Omega_{ci}^{-1} (v_{\perp}^2/2 + v_{\parallel}^2) / R$. Here Ω_{ci} is the ion cyclotron frequency, $v_{\perp, \parallel}$ are respectively the perpendicular and the parallel velocity of the ion, $\mu = v_{\perp}^2 / (2B)$ is the magnetic moment, $\hat{\mathbf{n}} = \mathbf{B} / |\mathbf{B}|$ is the versor of the magnetic field \mathbf{B} and R is the radius of curvature of the magnetic line. We introduce the notation v_{Di} , constant and positive. The sign of the velocity will be given according to the particular type

of ion's motion and according to the helical orientation of the magnetic field line. The latter is given by the direction of the plasma current, which we take in the following anti-parallel to the main magnetic field.

We consider first the trapped (t) ions that have, at the moment of ionization, parallel velocity in the same direction with the magnetic field ($+$ \parallel) and we note that their banana is entirely outside the magnetic surface on which the ionization has taken place. The ion radial displacement, on the length $d = \Delta^{t+} \approx$ half of the ion banana and only on the time interval of this displacement $\delta t = \Delta^{t+}/v_{Di}$, is toward the edge.

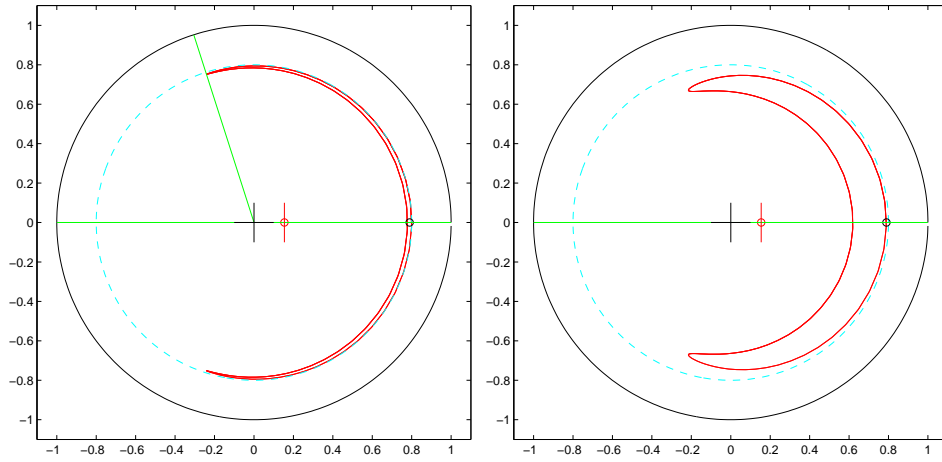


Figure 1: The banana orbit of an ion, which is fully inside the magnetic surface where it has been created. The magnetic surface is represented by the *cyan* dashed circle. The open black dot corresponds to the *center* of the positions $r(t)$. The open red dot (and the small red vertical line) indicate the *center* of the positions on the coordinate $x(t)$. Just for better visibility we show the orbit dilated along the radius by an arbitrary factor ($\times 10$).

The trapped ions that have in the point of ionization a velocity anti-parallel to the magnetic field vector, ($-$ \parallel) have banana orbit entirely inside the magnetic surface and the transitory displacement of the new ion, until the “center” of this banana, is towards smaller r radius, $d = -\Delta^{t-} < 0$ (where Δ^{t-} is defined positive).

In addition there are circulating (c) new ions, *i.e.* on untrapped orbits. Those that have at the initial point a momentum directed parallel to the magnetic field ($+$ \parallel) have a circular orbit which is entirely inside the magnetic surface on which the ionization has taken place. The effective displacement to the virtual center is toward larger radius, $d = \Delta^{c+} > 0$ (Δ^{c+} is defined positive).

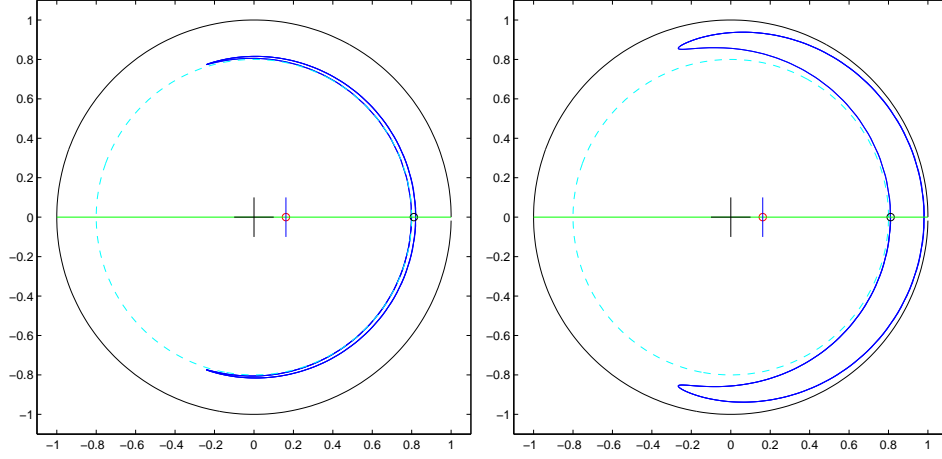


Figure 2: The banana orbit of an ion, which is outside the magnetic surface. The magnetic surface is represented by the *cyan* dashed circle. The open black dot corresponds to the *center* of the positions $r(t)$. The open red dot (and the small blue vertical line) indicate the *center* of the positions on the coordinate $x(t)$. Just for better visibility we show the orbit dilated along the radius by an arbitrary factor ($\times 10$).

The last type consists of ions that are circulating and with their velocity at the initial point anti-parallel to the magnetic field ($- \parallel$). For them the closed orbit fully includes the magnetic surface and it is equivalent to the displacement of the average position of the new ion to smaller r , toward the magnetic axis, $d = -\Delta^{c-} < 0$ (Δ^{c-} is defined positive).

The four contributions to the current through (r, t) , from the two pairs (*i.e.* $(\pm \parallel)$ -trapped, respectively $(\pm \parallel)$ -circulating) appear to be small and they partly compensate, having opposite signs. However, even the small remaining (effective) radial displacement, multiplied with the rate of generation of new ions, leads to a significant radial current. There is another aspect: the centers of the two bananas discussed above $[(+ \parallel)$ and $(- \parallel)]$ are spatially separated and we can associate to them the full population of new ions generated in those two positions. The rate of ionization, expressed in number of ions per m^3 per second has a significant radial variation, both for pellets and for gas-puff: the rate of generation of new ions may differ substantially between two radial positions, even if they have small separation, of the order of centimeters. The two banana centers are separated by a distance $\Delta^{t+} + \Delta^{t-}$ which is in this range and suggests that the radial variation of the rate of ionization is an important factor.

For any point r , the four contributions combine into a single, short-lived, finite-spatial

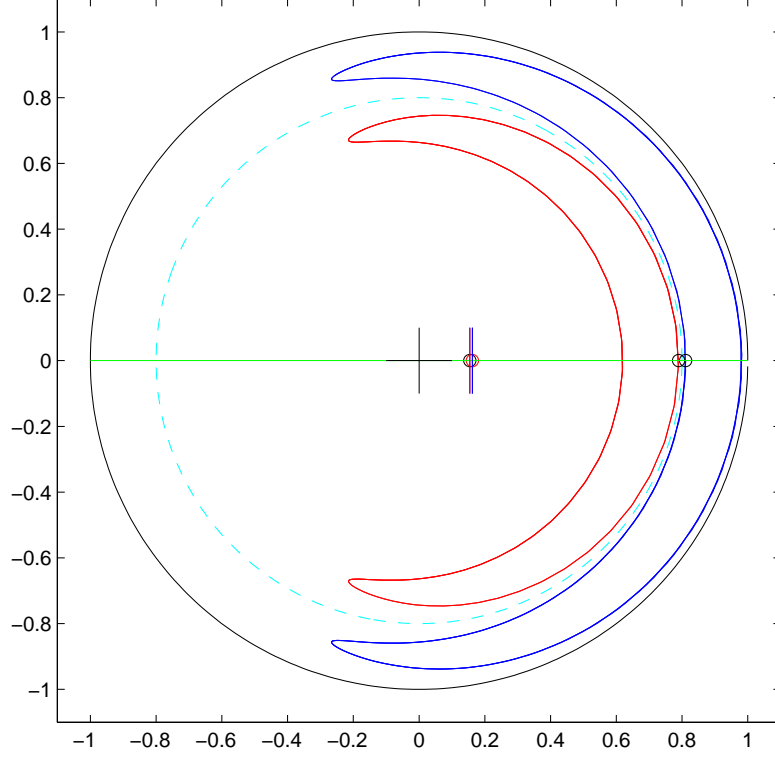


Figure 3: The banana orbits of two ions. One is inside (red) the other is outside (blue) the magnetic surface. The magnetic surface is represented by the *cyan* dashed circle. The two open black dots correspond to the *centers* of the positions $r(t)$, for each orbit. The two open red and black dots (and the small red and blue vertical lines) indicate the *centers* of the positions on the coordinates $x(t)$ for both orbits. For better visibility we multiply the radius coordinate of each orbit by an arbitrary factor ($\times 10$).

size - event of ion charge displacement, *i.e.* a current. These events occur everywhere within the radial segment of ionization and for all the time when there are still neutral atoms to be ionized.

B. Calculation of the flux of electric charge of the new ions into a point (r, t)

The pellet contains a total number of particles (neutral atoms) N_t and the ionization takes place in the toroidal volume between the surfaces r_1 and r_2 , $V_t = 2\pi^2 R(r_2^2 - r_1^2)$. The *total* time for ionization of the particles of the pellet is τ^{ioniz} . The rate of generation of ions

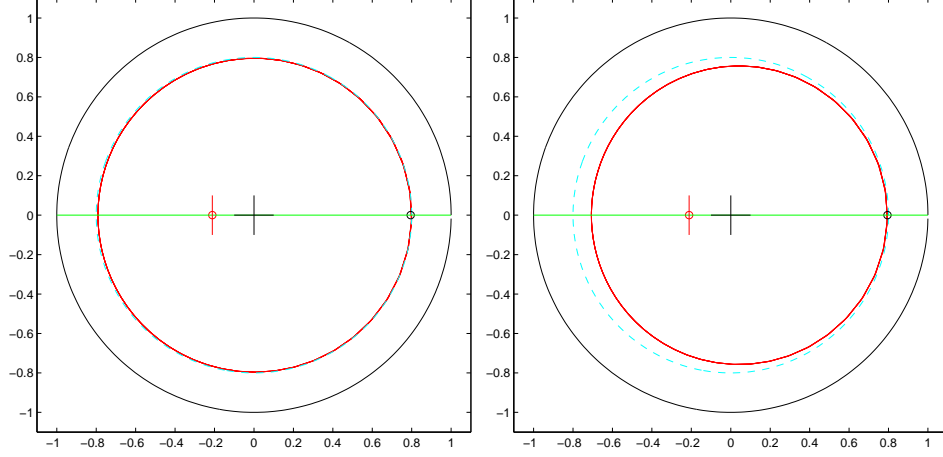


Figure 4: The untrapped (circulating) orbit of an ion, fully inside the magnetic surface. The magnetic surface is represented by the *cyan* dashed circle. The open black dot corresponds to the *center* of the positions $r(t)$. The open red dot (and the small red vertical line) indicate the *center* of the positions on the coordinate $x(t)$. Just for better visibility we also show the orbit dilated along the radius by an arbitrary factor ($\times 10$).

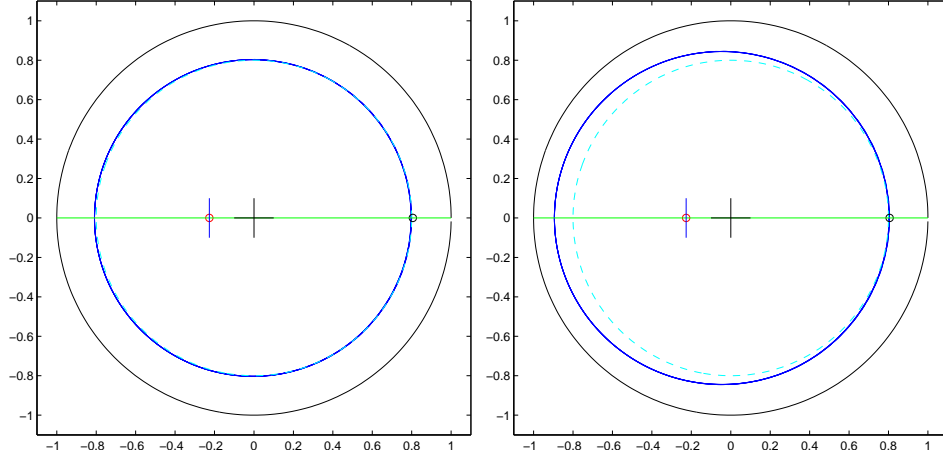


Figure 5: The untrapped (circulating) orbit of an ion, fully outside the magnetic surface. The magnetic surface is represented by the *cyan* dashed circle. The open black dot corresponds to the *center* of the positions $r(t)$. The open red dot (and the small red vertical line) indicate the *center* of the positions on the coordinate $x(t)$. Just for better visibility we show the orbit dilated along the radius by an arbitrary factor ($\times 10$).

per unit volume and per second has the average magnitude

$$\dot{n}^{ioniz}(r, t) \sim \frac{N_t}{\tau^{ioniz}} \frac{1}{V_t} \quad (1)$$

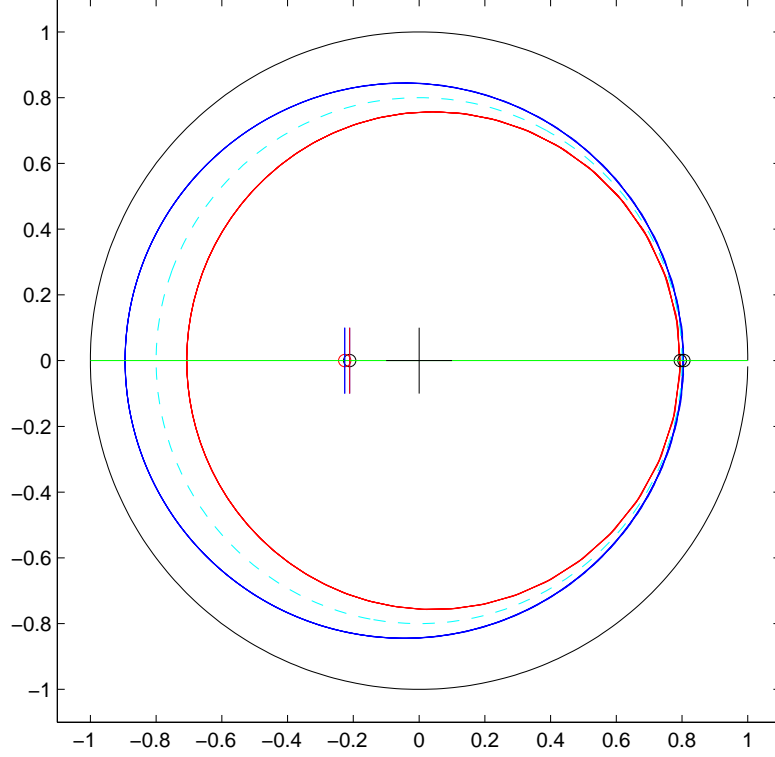


Figure 6: The untrapped (circulating) orbits of two ions fully enclosing (blue) respectively fully inside (red) the magnetic surface. The magnetic surface is represented by the *cyan* dashed circle. The two open black dots correspond to the *centers* of the positions $r(t)$, for each orbit. The two open red and black dots (and the small red and blue vertical lines) indicate the *centers* of the positions on the coordinates $x(t)$ for both orbits. For better visibility we multiply the radius coordinate of each orbit by an arbitrary factor ($\times 10$).

The rate of ionization has strong spatial and temporal variation and we find more convenient to express it as

$$\dot{n}^{ioniz}(r, t) = \dot{n}_0^{ioniz} S(r, t) \left(\frac{ions}{m^3 s} \right) \quad (2)$$

where $S(r, t) \geq 0$ is by definition a nondimensional function representing the space-time variation of the ionization rate. The maximum of S is 1 and its variable is normalized, $x \equiv r/a$. The constant factor \dot{n}_0^{ioniz} (of order $\sim 10^{23} ions/m^3/s$) is the physical quantity that carries information on the average rate of ionization and is taken from experimental observation. The factors \dot{n}_0^{ioniz} and S are constraint by the condition

$$\int_0^{\tau^{ioniz}} d\tau \int dV \dot{n}^{ioniz}(r, t) = N_t \quad (3)$$

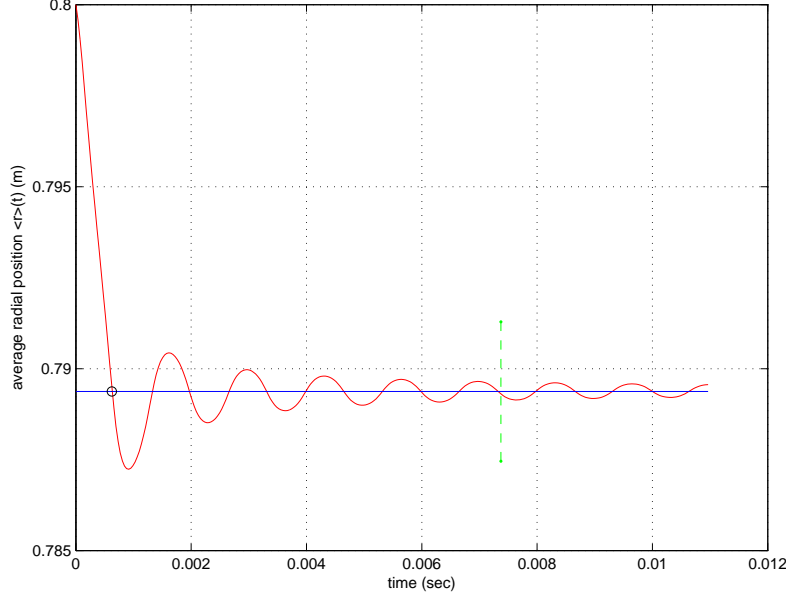


Figure 7: The time evolution of the average radial position $\bar{r}(t)$ for an ions whose orbit is fully inside the magnetic surface. The straight horizontal line is the asymptotic average position r_{asympt} (the “center” of the periodic orbit). The dashed vertical line in the asymptotic range is used to select the part of the trajectory to determine r_{asympt} , far from the transient. The open dot at the intersection of $r = r_{asympt}$ and $r = \bar{r}(t)$ determines the approximative end of the transitory regime, τ_{asympt} . The drift velocity is estimated as $v_{Di} = \frac{r_{asympt} - r_{ini}}{\tau_{asympt}}$, where r_{ini} is the radial position at ionization.

For example, taking for simplicity a source that is constant in time for the entire duration of the ionization $[0, \tau^{ioniz}]$, we have

$$\dot{n}_0^{ioniz} \tau^{ioniz} \int_{r_1}^{r_2} S(r) 4\pi^2 R r dr = N_t \quad (4)$$

The finite volume V_t is divided into toroidal shells of infinitesimal width dr on the minor radius, placed at the position r , with volume $V_{dr} = A dr = 4\pi^2 R r (dr)$ where A is the surface area. We fix a reference position $r \in [r_1, r_2]$, and calculate the net flux of ions that traverses the surface $A = 4\pi^2 R r$ at r . Consider the bunch of ions that are produced in a time $\delta\tau$, filling the elementary shell (denoted D) situated at a distance ρ from r . Their number is $\dot{n}^{ioniz} \left(r - \rho, t - \frac{\rho}{v_{Di}} \right) \times V_{dr} \delta\tau$. The ions from D that are generated at time $t - \rho/v_{Di}$ travel with constant velocity v_{Di} and arrive in r at time t , traversing the surface A in a time $\delta\tau$. The flux at (r, t) , in $(ions/m^2/s)$, is

$$\Gamma(r, t) = \dot{n}^{ioniz} \left(r - \rho, t - \frac{\rho}{v_{Di}} \right) V_{dr} \delta\tau \frac{1}{A} \frac{1}{\delta\tau} = \dot{n}^{ioniz} \left(r - \rho, t - \frac{\rho}{v_{Di}} \right) dr \quad (5)$$

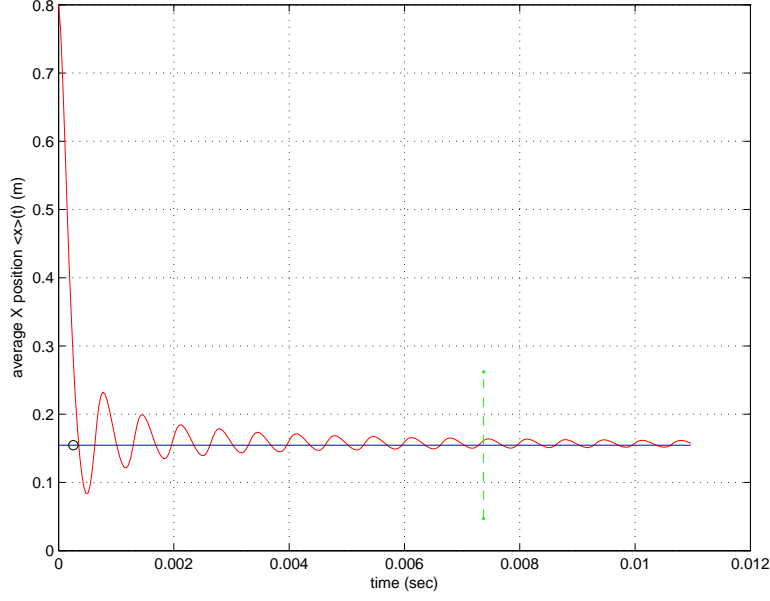


Figure 8: The time evolution of the average x -projection of the position, *i.e.* $\overline{x}(t)$, for an ions whose orbit is fully inside the magnetic surface. The details are the same as for Figure 7.

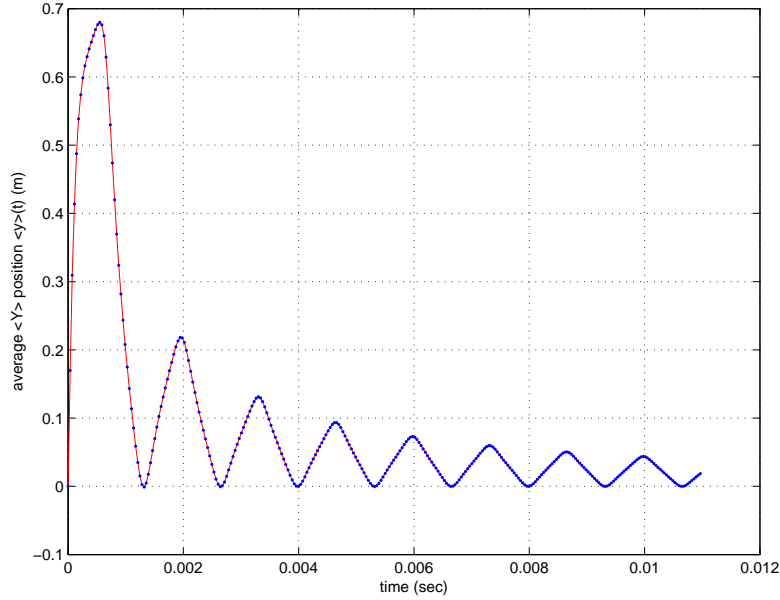


Figure 9: The time evolution of the average y -projection of the position, *i.e.* $\overline{y}(t)$, for an ions whose orbit is fully inside the magnetic surface. We note that it remains positive at all times.

The maximum distance of travel on which a new ion generates a current is from the point of ionization until the “center” of the periodic orbit, $\rho_{\max} = \Delta$ (which is one of $\Delta^{t\pm}$). Between $r - \Delta$ and r there are many infinitesimal shells, at distance ρ' from r ($\Delta \geq \rho' \geq 0$). The ions created in these intermediate cells arrive at time t in r if they are generated at $t - \rho'/v_{Di}$.

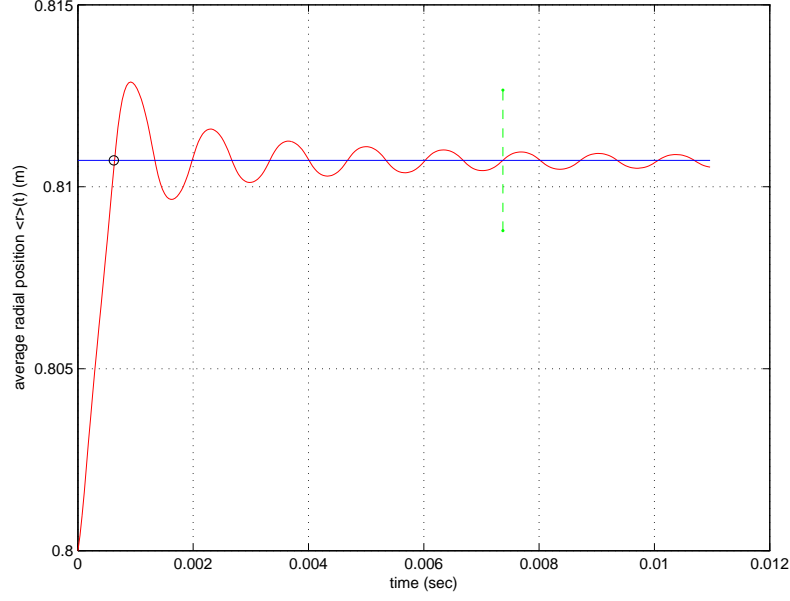


Figure 10: The time evolution of the average radial position $\bar{r}(t)$ for an ions whose orbit is outside the magnetic surface. The details are the same as for Figure 7.

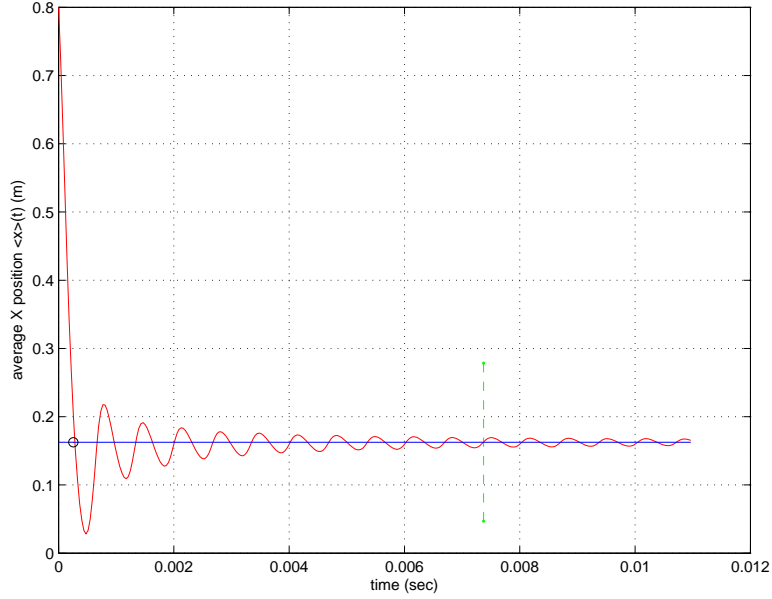


Figure 11: The time evolution of the average x -projection of the position, *i.e.* $\bar{x}(t)$, for an ions whose orbit is outside the magnetic surface. The details of the Figure are the same as for Figure 7.

Summing these partial contributions Eq.(5), the origins of which are in the interval $[r - \Delta, r]$

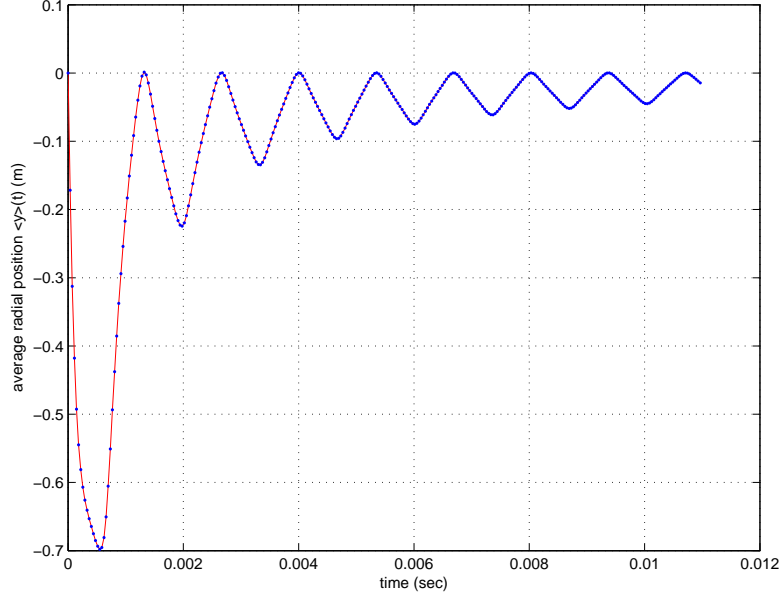


Figure 12: The time evolution of the average y -projection of the position, *i.e.* $\bar{y}(t)$, for an ions whose orbit is outside the magnetic surface.

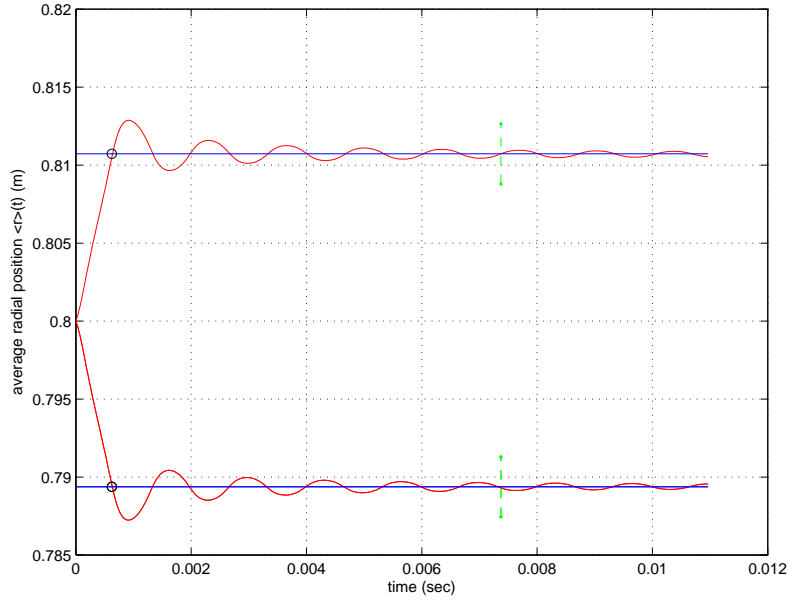


Figure 13: This plot represents the time evolutions of the average positions on r , *i.e.* $\bar{r}(t)$, for the trapped particles whose orbits are fully inside (lower curve) and respectively outside (the upper curve) the magnetic surface. The details are the same as in Figure 7.

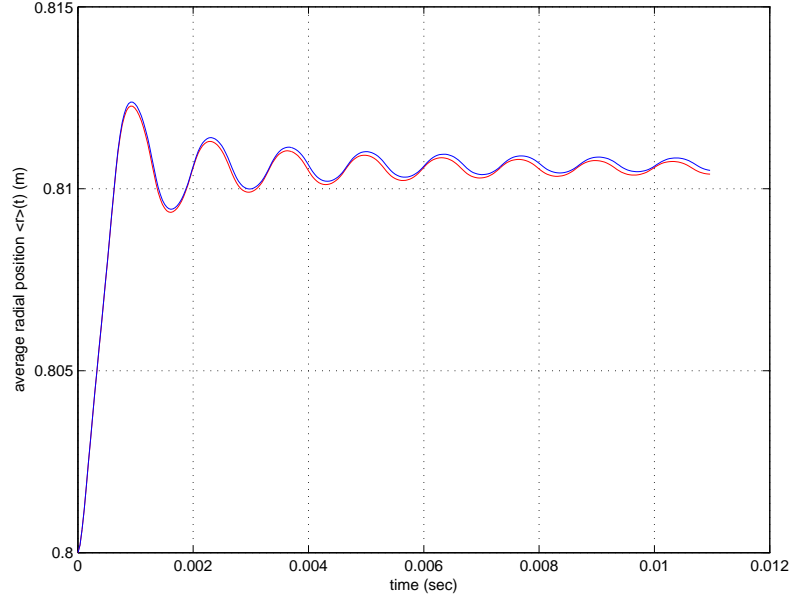


Figure 14: The time variation of the average positions on r , *i.e.* $\bar{r}(t)$, for the two types of trapped orbits are represented here with the purpose to give an idea of the smallness of the difference in the average radial displacements. One of the curves (the lower one in Figure 13) has been reversed in order to make easier the comparison.

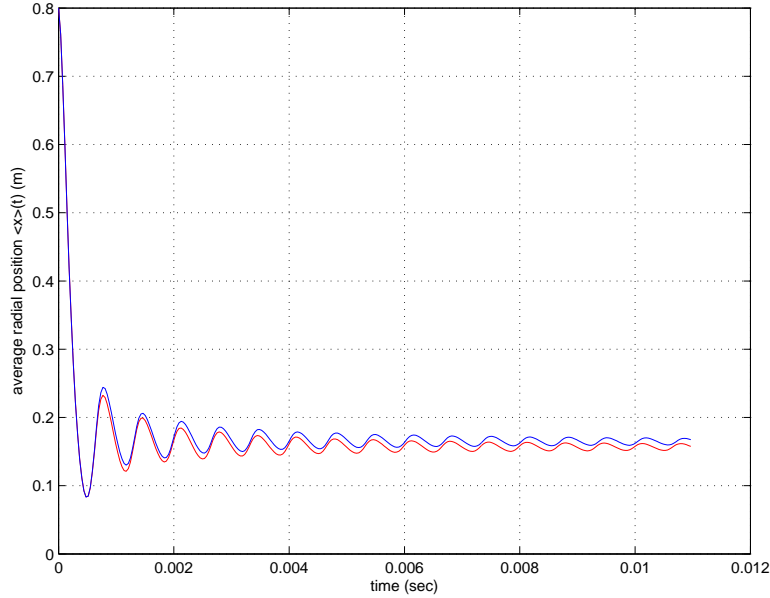


Figure 15: The same as Figure 14 but for the x -projection.

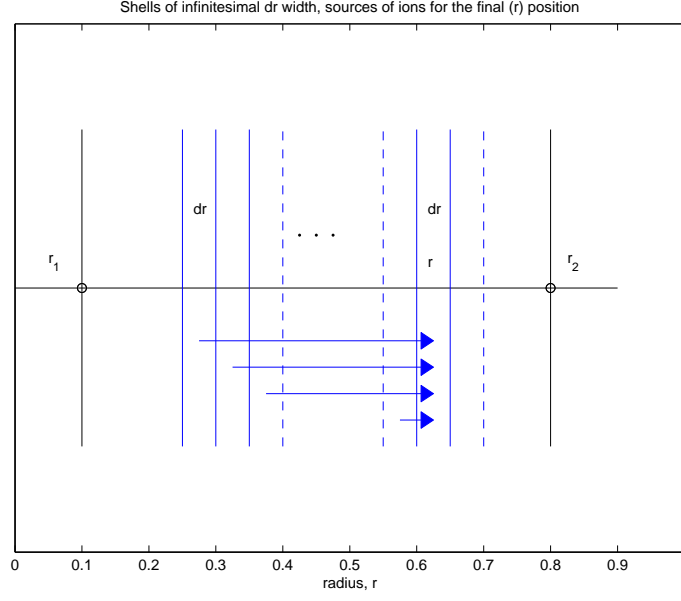


Figure 16: A simple representation of the fluxes that are traversing the surface placed at the radius r , coming from various infinitesimal regions δr . The sum over these contributions is the integral that defines the current density in (r, t) according to the text. The positions r_1 and r_2 are the limits of the domain of ionization.

it results $\Gamma^\Delta(r, t)$

$$\begin{aligned}
 \Gamma^\Delta(r, t) &= \int_0^\Delta n^{ioniz} \left(r - \rho', t - \frac{\rho'}{v_{Di}} \right) d\rho' \\
 &\approx n_0^{ioniz} \int_0^\Delta d\rho' \left[S(x, t) - \left(\frac{\partial S}{\partial r} \right) \rho' - \left(\frac{\partial S}{\partial t} \right) \frac{\rho'}{v_{Di}} \right] \\
 &= n_0^{ioniz} \left[S(r, t) \Delta - \frac{1}{2} \left(\frac{\partial S}{\partial r} \right) \Delta^2 - \frac{1}{2} \left(\frac{\partial S}{\partial t} \right) \frac{\Delta^2}{v_{Di}} \right]
 \end{aligned} \tag{6}$$

where the derivatives of S are calculated in (r, t) . This flux must be multiplied with the fractional number representing how many of the new ions will settle on trapped, respectively circulating orbits. We take the approximative values $\sqrt{\varepsilon}$ and respectively $1 - \sqrt{\varepsilon}$. In addition, we assume that a fraction of $1/2$ new ions have parallel, respectively anti-parallel initial velocities.

C. The current density in (r, t)

Taking into account the four type of ion's orbits, we use Eq.(6) to estimate the flows of new ions coming in, or leaving, the point (r, t) . The contributions from neighbor points are

$$\begin{aligned}\Gamma_{in}^{t(+||)}(r, t) &= \frac{1}{2}\sqrt{\varepsilon} \int_0^{\Delta^{t+}} \dot{n}^{ioniz} \left(r - \rho', t - \frac{\rho'}{v_{di}} \right) d\rho' \\ &= \frac{1}{2}\sqrt{\varepsilon} \dot{n}_0^{ioniz} \left[S(r, t) \Delta^{t+} - \frac{1}{2} \left(\frac{\partial S}{\partial r} \right) (\Delta^{t+})^2 - \frac{1}{2} \left(\frac{\partial S}{\partial t} \right) \frac{(\Delta^{t+})^2}{v_{Di}} \right]\end{aligned}\quad (7)$$

This is the number of ions that are trapped and had an initial velocity parallel with \mathbf{B} . They are produced in $\left(r - \rho', t - \frac{\rho'}{v_{Di}} \right)$, summed over $[r - \Delta^{t+}, r]$, and flow toward (r, t) from the left (*i.e.* their current is positive).

$$\begin{aligned}\Gamma_{in}^{t(-||)}(r, t) &= \frac{1}{2}\sqrt{\varepsilon} \int_0^{\Delta^{t-}} \dot{n}^{ioniz} \left(r + \rho', t - \frac{\rho'}{v_{di}} \right) d\rho' \\ &= \frac{1}{2}\sqrt{\varepsilon} \dot{n}_0^{ioniz} \left[S(r, t) \Delta^{t-} + \frac{1}{2} \left(\frac{\partial S}{\partial r} \right) (\Delta^{t-})^2 - \frac{1}{2} \left(\frac{\partial S}{\partial t} \right) \frac{(\Delta^{t-})^2}{v_{Di}} \right]\end{aligned}\quad (8)$$

This is the number of ions that are trapped and had an initial velocity anti-parallel to \mathbf{B} . They are produced in $\left(r + \rho', t - \frac{\rho'}{v_{Di}} \right)$, summed over the interval $[r, r + \Delta^{t-}]$ and flow towards (r, t) from the right (*i.e.* their current is negative).

$$\begin{aligned}\Gamma_{in}^{c(+||)}(r, t) &= \frac{1}{2} (1 - \sqrt{\varepsilon}) \int_0^{\Delta^{c+}} \dot{n}^{ioniz} \left(r - \rho', t - \frac{\rho'}{v_{di}} \right) d\rho' \\ &= \frac{1}{2} (1 - \sqrt{\varepsilon}) \dot{n}_0^{ioniz} \left[S(r, t) \Delta^{c+} - \frac{1}{2} \left(\frac{\partial S}{\partial r} \right) (\Delta^{c+})^2 - \frac{1}{2} \left(\frac{\partial S}{\partial t} \right) \frac{(\Delta^{c+})^2}{v_{Di}} \right]\end{aligned}\quad (9)$$

This is the number of ions that are circulating and had an initial velocity parallel with \mathbf{B} . They are produced in $\left(r - \rho', t - \frac{\rho'}{v_{Di}} \right)$, summed over the interval $[r - \Delta^{c+}, r]$ and flow towards (r, t) from the left (*i.e.* their current is positive).

$$\begin{aligned}\Gamma_{in}^{c(-||)}(r, t) &= \frac{1}{2} (1 - \sqrt{\varepsilon}) \int_0^{\Delta^{c-}} \dot{n}^{ioniz} \left(r + \rho', t - \frac{\rho'}{v_{di}} \right) d\rho' \\ &= \frac{1}{2} (1 - \sqrt{\varepsilon}) \dot{n}_0^{ioniz} \left[S(r, t) \Delta^{c-} + \frac{1}{2} \left(\frac{\partial S}{\partial r} \right) (\Delta^{c-})^2 - \frac{1}{2} \left(\frac{\partial S}{\partial t} \right) \frac{(\Delta^{c-})^2}{v_{Di}} \right]\end{aligned}\quad (10)$$

This is the number of ions that are circulating and had an initial velocity anti-parallel to \mathbf{B} . They are produced in $\left(r + \rho', t - \frac{\rho'}{v_{Di}} \right)$, summed over $[r, r + \Delta^{c-}]$ and flow towards (r, t) from the right (*i.e.* their current is negative).

The current density resulting from the *in* fluxes is

$$J^{in}(x, t) = |e| \left(\Gamma_{in}^{t(+||)} - \Gamma_{in}^{t(-||)} + \Gamma_{in}^{c(+||)} - \Gamma_{in}^{c(-||)} \right) \quad (11)$$

or

$$\begin{aligned} J^{in}(x, t) &= \frac{1}{2} |e| n_0^{\cdot ioniz} \left\{ S(x, t) \left[\sqrt{\varepsilon} \Delta^{t+} - \sqrt{\varepsilon} \Delta^{t-} + (1 - \sqrt{\varepsilon}) \Delta^{c+} - (1 - \sqrt{\varepsilon}) \Delta^{c-} \right] \right. \\ &\quad + \frac{1}{2} \left(\frac{\partial S}{\partial r} \right) \left[-\sqrt{\varepsilon} (\Delta^{t+})^2 - \sqrt{\varepsilon} (\Delta^{t-})^2 - (1 - \sqrt{\varepsilon}) (\Delta^{c+})^2 - (1 - \sqrt{\varepsilon}) (\Delta^{c-})^2 \right] \\ &\quad \left. + \frac{1}{2} \frac{1}{v_{Di}} \left(\frac{\partial S}{\partial t} \right) \left[-\sqrt{\varepsilon} (\Delta^{t+})^2 + \sqrt{\varepsilon} (\Delta^{t-})^2 - (1 - \sqrt{\varepsilon}) (\Delta^{c+})^2 + (1 - \sqrt{\varepsilon}) (\Delta^{c-})^2 \right] \right\} \end{aligned} \quad (12)$$

We now have to calculate the flows (*out*) that leave the shell of the point (r, t) . The groups that are leaving (r, t) are:

Trapped with parallel (*i.e.* positive) initial velocity $t(+||)$

$$n_{out}^{t(+||)}(r, t) = \frac{1}{2} \sqrt{\varepsilon} n^{\cdot ioniz}(r, t) \quad (\text{toward large } r) \quad (13)$$

The second group consists of trapped with anti-parallel (*i.e.* negative) initial velocity

$$n_{out}^{t(-||)}(r, t) = \frac{1}{2} \sqrt{\varepsilon} n^{\cdot ioniz}(r, t) \quad (\text{toward small } r) \quad (14)$$

The third group consists of circulating ions with parallel initial velocity

$$n_{out}^{c(+||)}(r, t) = \frac{1}{2} (1 - \sqrt{\varepsilon}) n^{\cdot ioniz}(r, t) \quad (\text{toward large } r) \quad (15)$$

The fourth group consists of circulating ions with anti-parallel initial velocity

$$n_{out}^{c(-||)}(r, t) = \frac{1}{2} (1 - \sqrt{\varepsilon}) n^{\cdot ioniz}(r, t) \quad (\text{toward small } r) \quad (16)$$

Summing the *out* components after taking into account the signs according to the description

$$J^{out}(r, t) = |e| \left(\Gamma_{out}^{t(\\|)} - \Gamma_{out}^{t(-\\|)} + \Gamma_{out}^{c(\\|)} - \Gamma_{out}^{c(-\\|)} \right) = 0 \quad (17)$$

Adding the flows *in* and *out* $J(r, t) = J^{in}(r, t) - J^{out}(r, t)$ we obtain

$$\begin{aligned} J(r, t) &= \frac{1}{2} |e| n_0^{\cdot ioniz} \left\{ S(r, t) \left[\sqrt{\varepsilon} (\Delta^{t+} - \Delta^{t-}) + (1 - \sqrt{\varepsilon}) (\Delta^{c+} - \Delta^{c-}) \right] \right. \\ &\quad + \frac{1}{2} \left(\frac{\partial S}{\partial r} \right) \left[-\sqrt{\varepsilon} \left((\Delta^{t+})^2 + (\Delta^{t-})^2 \right) - (1 - \sqrt{\varepsilon}) \left((\Delta^{c+})^2 + (\Delta^{c-})^2 \right) \right] \\ &\quad \left. + \frac{1}{2} \frac{1}{v_{Di}} \left(\frac{\partial S}{\partial t} \right) \left[\sqrt{\varepsilon} \left(-(\Delta^{t+})^2 + (\Delta^{t-})^2 \right) + (1 - \sqrt{\varepsilon}) \left(-(\Delta^{c+})^2 + (\Delta^{c-})^2 \right) \right] \right\} \end{aligned} \quad (18)$$

We show in **Appendix A** that the contributions of the circulating ions is much smaller than that of the trapped ions and for the present estimation can be neglected

$$J(r, t) \approx \frac{1}{2} |e| \dot{n}_0^{ioniz} \left\{ S(x, t) \sqrt{\varepsilon} [\Delta^{t+} - \Delta^{t-}] - \frac{1}{2} \left(\frac{\partial S}{\partial r} \right) \sqrt{\varepsilon} [(\Delta^{t+})^2 + (\Delta^{t-})^2] + \frac{1}{2} \frac{1}{v_{Di}} \left(\frac{\partial S}{\partial t} \right) \sqrt{\varepsilon} [-(\Delta^{t+})^2 + (\Delta^{t-})^2] \right\} \quad (19)$$

In the numerical model (next Section) we take a time-independent source, $\partial S / \partial t = 0$, and the current density becomes

$$J(r) \approx \frac{1}{2} |e| \dot{n}_0^{ioniz} \sqrt{\varepsilon} \left\{ S(r, t) (\Delta^{t+} - \Delta^{t-}) - \frac{1}{2} \left(\frac{\partial S}{\partial r} \right) [(\Delta^{t+})^2 + (\Delta^{t-})^2] \right\} \quad (20)$$

The distance Δ^{\pm} travelled by the new ion from ionization to the “center” of the periodic motion (*i.e.* the distance on which there is effective current) will be calculated in the next Section by solving the equations of motion of the ion, as initial value problem. For the present estimation we adopt neoclassical approximations⁷ replacing Δ^{\pm} with the “radius” of the banana,

$$\Delta^{\pm} \approx v_{Di} \tau_{bounce} = \rho_i q \varepsilon^{-1/2} \quad (21)$$

where ions $v_{Di} \approx \frac{1}{\Omega_{ci}} \frac{v_{th,i}^2}{R}$ and $\tau_{bounce} \approx r / v_{\theta} = \frac{r B}{B_{\theta}} \frac{1}{v_{th,i}} \sqrt{\frac{R}{r}}^{22}$. In regions where the ionization rate has strong spatial variation, the second term in Eq.(20) is large and we can simplify the result as

$$J \approx -\frac{1}{2} |e| \dot{n}_0^{ioniz} \left(\frac{\partial S}{\partial r} \right) \rho_i^2 q^2 \varepsilon^{-1/2} \quad (22)$$

For an estimation we take $a = 1$ (m), $R = 3.5$ (m), $B_T = 3.5$ (T), $T_i = 1.5$ (keV), $N_t = 3 \times 10^{21}$ neutral atoms in the pellet, $\tau^{ioniz} \approx 4 \times 10^{-3}$ (s) duration of the complete ionization process^{1, 16} and the radial extension of the zone of ionization is between $r_1 = 0.4a$ and $r_2 = 0.7a$. The energy of the new ions is a fraction ($\eta = 0.75$) of the background ion energy and the trapping parameter $\lambda = h v_{\perp}^2 / v^2$, $h = 1 + \varepsilon \cos \theta$ is taken $\lambda = 0.92$. It results $V_t \approx 22.8$ (m³), $A(r) \approx 138r$ (m²) and the average rate of ionization $\dot{n}_0^{ioniz} \sim 3.3 \times 10^{22}$ (ions/m³/s). Adopting for $S(r)$ a simple spatial profile limited between $r_a = 0.475a$, $r_b = 0.625a$, with $\max S = 1$ we find from the constraint Eq.(4) $\dot{n}_0^{ioniz} \approx 1.2 \times 10^{23}$ (ions/m³/s). Using values suggested by experiments^{16, 13, 3, 2, 1}, Δ^{\pm} from exact integration, and $a^{-1} \partial S / \partial x \sim 20$ (m⁻¹), we obtain from Eq.(20) $|J| \sim 11.52$ (A/m²).

The result is indeed high. For comparison we consider $nm_i \partial v_\theta / \partial t \sim JB_T$. This means $\partial v_\theta / \partial t \sim 23 \times 10^8 \text{ (m/s}^2\text{)}$, or, in every microsecond the poloidal speed would increase with more than 4 (km/s) . In less than one tenth of a milliseconds v_θ rises to the range of the ion thermal speed $v_{th,i} \sim 0.38 \times 10^3 \text{ (km/s)}$. For comparison the transit time magnetic pumping decay of the poloidal velocity would contribute with

$$-\gamma^{MP} = \frac{\partial}{\partial t} \ln v_\theta = \frac{3}{4} \left(1 + \frac{1}{2q^2}\right) \left(\frac{l}{qR}\right)^2 \nu_{ii} \quad (23)$$

where l is the mean free path and ν_{ii} is the ion-ion collision time¹⁰. We find $-\gamma^{MP} \sim 1.2 \times 10^4 \text{ (s}^{-1}\text{)}$, and taking a poloidal velocity (as observed in some experiments, *e.g.*⁴) $v_\theta \sim 10^4 \text{ (m/s)}$ it is estimated $\left|(\partial v_\theta / \partial t)^{MP}\right| \sim 1.2 \times 10^8 \text{ (m/s}^2\text{)}$. It results

$$\left(\frac{\partial v_\theta}{\partial t}\right)^{ioniz} > \left|\left(\frac{\partial v_\theta}{\partial t}\right)^{MP}\right| \quad (24)$$

Of course, this ionization torque acts for short time (few milliseconds) and Eq.(22) is an overestimation as long as the neutral atoms' dynamics (*e.g.* the pellet cloud) and the bulk ion's reaction (return current) are not described in detail. But this result is a strong suggestion that the ionization torque is important.

III. NUMERICAL IMPLEMENTATION

The numerical simulation of this process has been done on a discrete mesh $\{r_i\}_{i=1,NX} \times \{t_k\}_{k=1,NT}$ for $NR = NT = 500$. The simple physical picture described above has been implemented.. For any cell (r_i, t_k) we calculate the number of ions that are generated, $\dot{n}_0^{ioniz} S(r, t)$, using the expression for $S(r) = \alpha + \beta(r/a) + \gamma(r/a)^2$. Imposing $S(r_a) = S(r_b) = 0$ and $\max S = 1$ at $(r_a + r_b)/2$, the coefficients are determined and, as explained above, Eq.(4) determines the constant $\dot{n}_0^{ioniz} = 1.2 \times 10^{23} \text{ (ions/m}^3\text{/s)}$. We now assume that the energy of the new ions is a fraction (0.75) of the background ion thermal energy (at $T_i = 1.5 \text{ keV}$) and that the probability of being trapped is $\sqrt{\varepsilon}$. Finally we assume that the probability that the ion has an initial velocity which is parallel to \mathbf{B} is 1/2, equal with the probability to be anti-parallel. Now we look at the way the ions move. The total excursion on r is Δ^{t+} (to larger r) and Δ^{t-} (to smaller r). The displacement is represented on the mesh $\{r_{i'}, t_{k'}\}$ and every cell (i', k') which is traversed by the flux of ions stores

this contribution, adding it to a variable that will finally be the current flowing through it. There are several other cells whose new ions traverse this cell (i', k') and all contributions are counted and summed. Due to the assumed constancy of v_{Di} , there is no decay along the path that starts from (r_i, t_k) and ends in the cell $(r_i + \Delta^{t+}, t + \Delta^{t+}/v_{Di})$, [respectively $(r_i - \Delta^{t-}, t + \Delta^{t-}/v_{Di})$ for the anti-parallel initial velocity]. All cells traversed along this path retain the contribution from (r_i, t_k) .

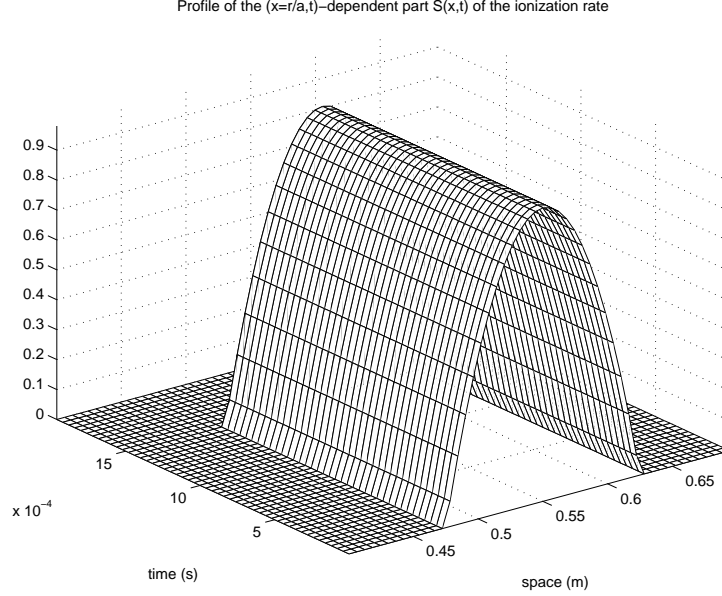


Figure 17: The space-time profile of the ionization source, the function $S(r, t)$. The factor \dot{n}_0 (ions/m³/s) multiplies this function to obtain the effective rate of production of new ions.

Instead of the neoclassical approximations for $\Delta^{t\pm}$ and v_{Di} ²² we choose to solve the system of equations of motion^{18, 5, 9, 31, 7} in every cell $(r_i, t_k)_{i=1, NX; k=1, NT}$.

$$\begin{aligned}\frac{dr}{dt} &\approx -\frac{1}{\Omega} \left(\frac{v_{\perp}^2}{2} + v_{\parallel}^2 \right) \frac{\sin \theta}{R_0} \\ \frac{d\theta}{dt} &\approx \frac{v_{\parallel}}{qR_0} - \frac{1}{r} \frac{1}{\Omega} \left(\frac{v_{\perp}^2}{2} + v_{\parallel}^2 \right) \frac{\cos \theta}{R_0} \\ \frac{d\varphi}{dt} &\approx \frac{v_{\parallel}}{R_0} \\ \frac{d}{dt} \left(\frac{v_{\perp}^2}{2} \right) &= \left(\frac{v_{\perp}^2}{2} \right) v_{\parallel} \frac{B_{\theta}}{B_T} \frac{\sin \theta}{R_0} \\ \frac{dv_{\parallel}}{dt} &= - \left(\frac{v_{\perp}^2}{2} \right) \frac{B_{\theta}}{B_T} \frac{\sin \theta}{R_0}\end{aligned}$$

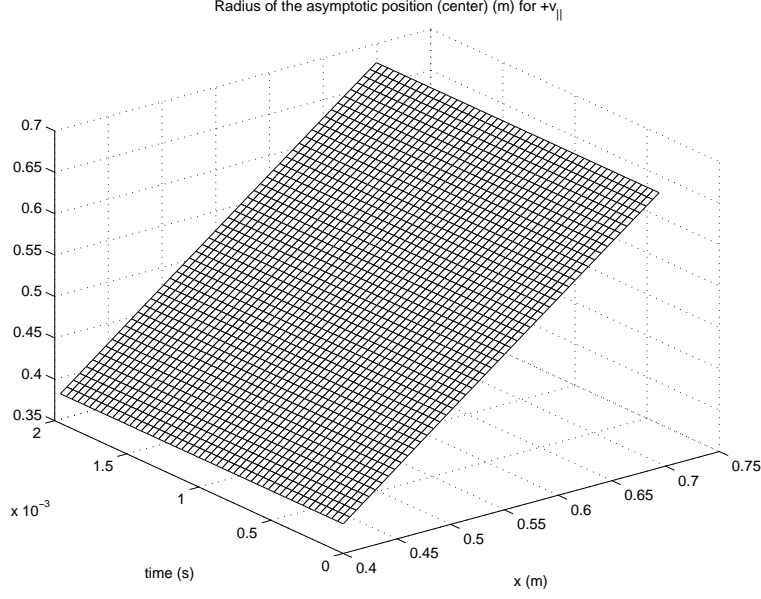


Figure 18: The (r, t) profile of the final position (the “center”) of the average $r(t)$ for the ions whose orbit encloses the magnetic surface. This is calculated by solving in every (r_i, t_k) , for $i = 1, NR, k = 1, NTIME$ cell of the discrete mesh, the set of equations of motion for a trapped ion.

From the solution we get the exact orbit of an ion born in the cell $(r_i, t_k)_{i=1, NR; k=1, NT}$ but we still have to operate the separation of the transitory part, the part which represents the unique manifestation of a current, from the periodic part of the trajectory, whose average does not produce a current. We calculate for each trajectory the time-dependent average position $\bar{r}(t) = \frac{1}{t} \int_0^t r(t') dt'$ and leave the integration sufficiently long such that the asymptotic quasi-static average position $r_{asympt} = \bar{r}(t \rightarrow \infty)$ to be clearly identified. This position r_{asympt} (the “center” of the banana) is retained and the quantity Δ^t is obtained as the difference between r_{asympt} and the initial position, which is the point of the ionization, r_{ini} . We still need the estimation of the *effective* time that is necessary for the ion to reach this asymptotic position. The first intersection between the asymptotic line $r = r_{asympt}$ and the evolution line $\bar{r}(t)$ takes place at a moment t_{asympt} , which is retained as the representative time of ion’s travel to the center. This procedure is admittedly approximative but we have tried several reasonably alternative methods and the present one seems the best.

Once we know $r_{asympt} - r_{ini} \equiv \Delta$ and t_{asympt} we find $v_{Di} = \Delta/t_{asympt}$ and all data for the displacements of the new ions originating from (r_i, t_k) on the mesh are now available. In every cell the system is solved for both parallel and anti-parallel initial velocities and

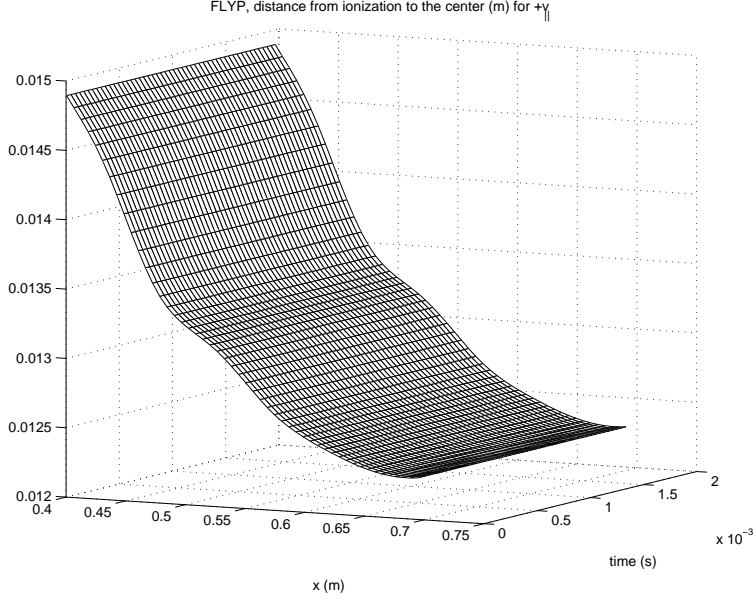


Figure 19: The variable $FLYP$, difference between the final position (the “center” of the banana) and the initial radial position (where ionization occurs) for an ions whose orbit encloses the magnetic surface. This is the amount of radial displacement of the ion on which there is current.

we calculate the distances $\Delta^{t\pm}$, the times t_{asympt}^{\pm} of this excursion and the drift velocities $v_{Di}^{\pm} = \Delta^{t\pm}/t_{asympt}^{\pm}$. This is shown in Figure 1 for ions with parallel, respectively anti-parallel initial velocity. The asymptotic position r_{asympt} is obtained by averaging a set of late values of $\bar{r}(t)$, for t beyond the vertical dashed lines. This ensures a good precision of identification of the “center”. The straight line $r = r_{asympt}$ intersects the evolution line $\bar{r}(t)$ is a point marked by a open dot, the time t_{asympt} .

We have adopted a profile $S(r)$ which is constant in time, Figure 2. Its support is $[r_a, r_b]$ inside the interval $[r_1, r_2]$. The empty radial regions on both sides are necessary because the excursions of lengths $\Delta^{t\pm}$ of the ions generated at the ends of the support must be recorded in these regions. The result (the current $J(r, t)$) depends on time since the process that starts at $t = 0$ (no-ionization) rises slowly by accumulating current contributions, before saturation. More interesting is the spatial profile confirming that the sign of $\partial S/\partial r$ is decisive and that the total torque, *i.e.* integrated over the plasma volume, is zero, as expected from conservation of angular momentum and from the fact that no ion is lost from plasma in our picture. The current is plotted in Figure 3. In Figure 4 we show the mesh-cells that contribute to the current calculated in a reference cell, chosen arbitrarily in

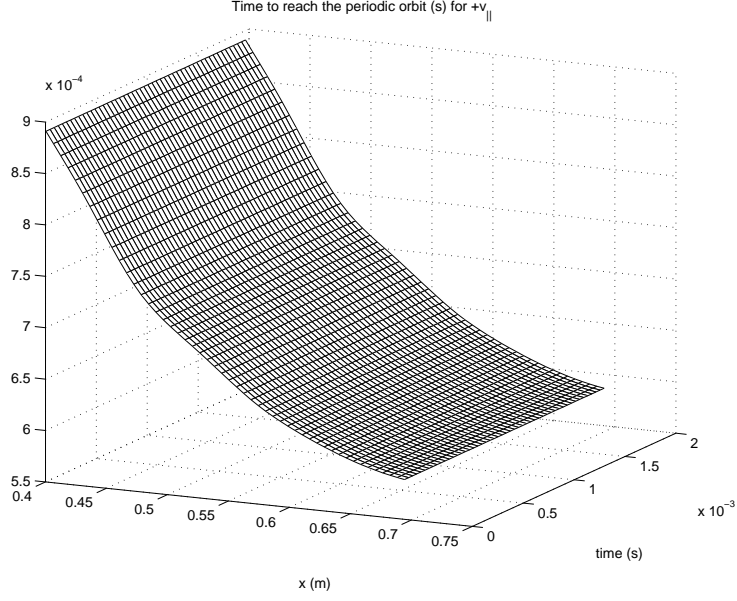


Figure 20: The (r, t) profile of the calculated time for an ion to reach the average position (the “center”) starting from the place of ionization.

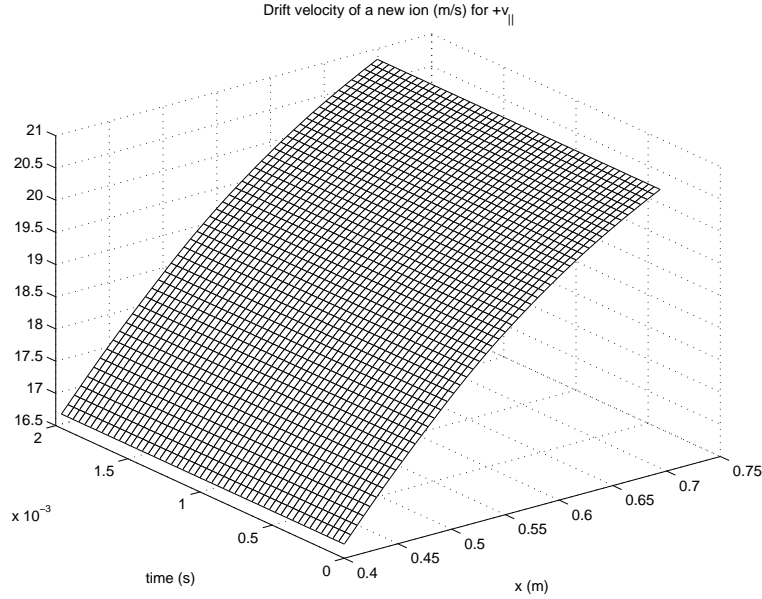


Figure 21: The (r, t) profile of the calculated drift velocity v_{Di} , as explained in Figure 7.

$(r, t) \equiv (ix = 350, itime = 150)$. The dots aligned on the a straight line (since $v_{Di} = \text{const}$) at left represent cells from where the new ions with positive (parallel) initial velocity arrive in r at t . The straight line at right represents ions with anti-parallel initial velocity.

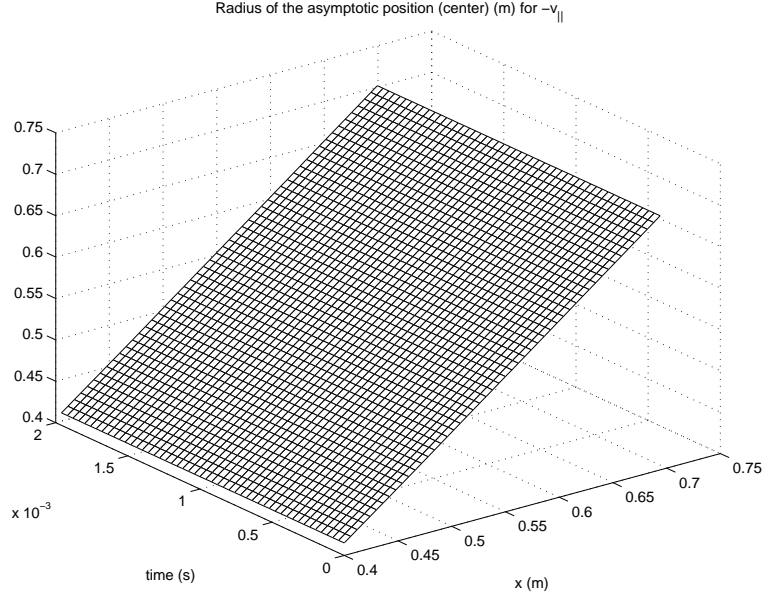


Figure 22: Same as Figure 18, but for ions whose orbits, calculated in every mesh-cell, are inside the magnetic surface.

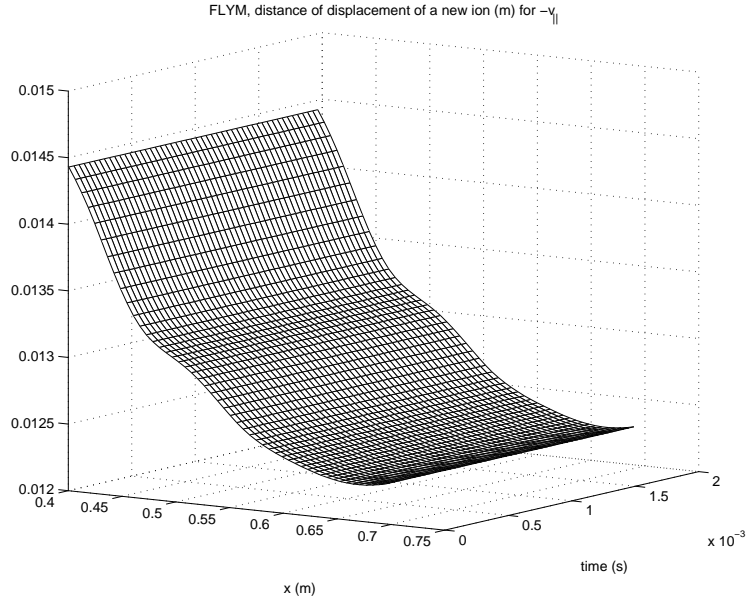


Figure 23: The variable $FLYM$, similar with $FLYP$ from Figure 19, but for the “smaller” banana.

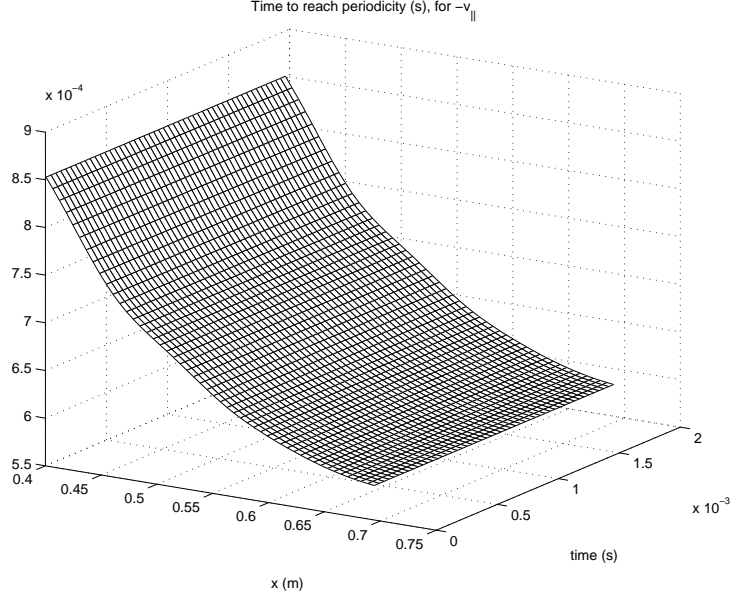


Figure 24: The time to reach the “center”, for the “smaller” banana.

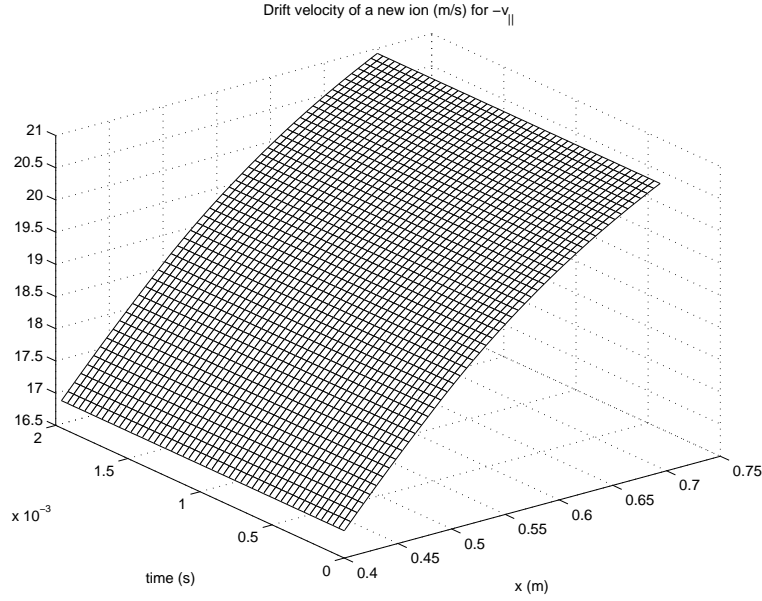


Figure 25: The drift velocity for the smaller banana.

IV. DRIFT-KINETIC CALCULATION OF THE IONIZATION-INDUCED CURRENT DENSITY

Similar problems are treated in the Ref.²³ (for alpha particles) and the Ref.¹² (for NBI). For the present case the drift-kinetic equation for the *new* ions, is

$$\frac{\partial f}{\partial t} + (v_{\parallel} \hat{\mathbf{n}} + \mathbf{v}_{Di}) \cdot \nabla f = S^{ioniz} \quad (25)$$

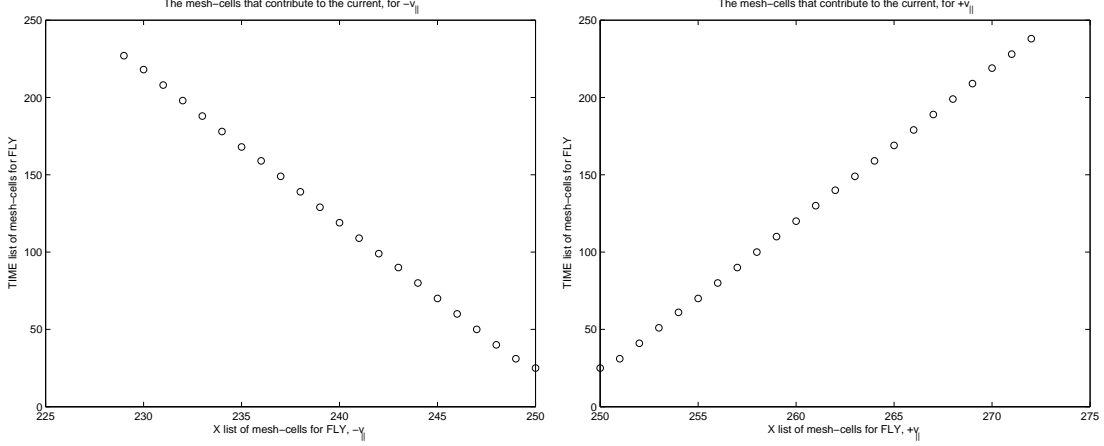


Figure 26: At left: the mesh-cells that are traversed by the ions generated in the point $(ir = 250, itime = 25)$ that evolve towards smaller radii (their banana orbits are fully inside the magnetic surface). At right: the mesh-cells that are traversed by the ions that evolve towards larger radii (their banana orbit ecloses the magnetic surface).

where the drift velocity of the guiding centre is $\mathbf{v}_{Di} = -v_{\parallel} \hat{\mathbf{n}} \times \nabla \left(\frac{v_{\parallel}}{\Omega_{ci}} \right)$ and the neoclassical notations will be used: $\xi = v_{\parallel}/v = (1 - \lambda/h)^{1/2}$, $\lambda = hv_{\perp}^2/v^2$, $h = 1 + \varepsilon \cos \theta$. The *limits* of the trapped particle region in the variable λ are $1 - \frac{r}{R} < \lambda < 1 + \frac{r}{R}$. The velocity space variables are v, λ and σ ($=\text{sign of } v_{\parallel}$).

Since in this simple treatment we neglect the effect of collisions the neoclassical small parameter is the ratio of the banana half-width to the minor radius, $\delta = \Delta^{\pm}/a \ll 1$. In usual neoclassical perturbative solution of the drift kinetic equation the zero order distribution function is the Maxwellian. In the present case, the perturbative expansion of f , the solution of the drift-kinetic equation for the new ions, must contain a term which is directly related to the source and, since this is determined by external factors, it cannot be ordered as powers of δ . The first term is formally of order -1 , f_{-1} .

$$f = f_{-1} + f_0 + f_1 + \dots \quad (26)$$

The lowest order

$$\hat{\mathbf{n}} \cdot \nabla f_{-1} = 0 \quad (27)$$

shows that f_{-1} is constant along the magnetic lines, or $f_{-1} = f_{-1}(\psi)$. This result is connected with an assumption about the distribution of ionization processes in space: they have a rate which is constant on a magnetic surface.

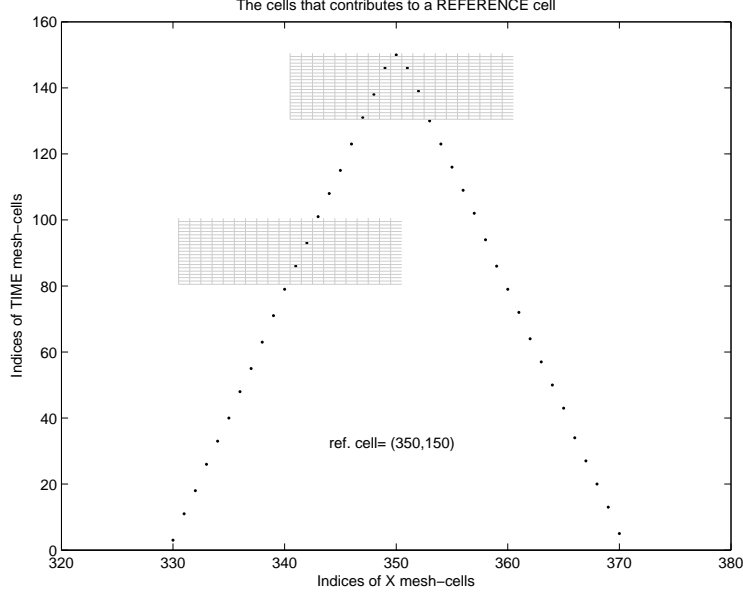


Figure 27: The mesh-cells that contribute to the current density that is “measured” in a reference cell (r, t) , with indices of discretization $ir = 350$ and $itime = 150$. From the cells that are marked by a dot the ions are moving to larger radii (for the dots that are at the left of the axis of symmetry of the figure) and respectively to smaller radii (for the dots that are at the right of the axis of symmetry). Accordingly the contributions must have been generated by ionization in a position $r - \rho$ and respectively $r + \rho$, and at a time $t - \rho/v_{Di}$, for them to reach the reference cell at (r, t) . The real mesh is too detailed to be shown and only two patches are shown, for illustration.

The zeroth order equation is

$$v_{\parallel} \hat{\mathbf{n}} \cdot \nabla f_0 = -\mathbf{v}_{Di} \cdot \nabla \psi \frac{\partial f_{-1}}{\partial \psi} - \frac{\partial f_{-1}}{\partial t} + S^{ioniz} \quad (28)$$

As in any multiple space-time scale analysis we average at this level (0) to obtain a solution on the level (-1) . We apply the operator of bounce averaging to eliminate the function f_0 . This gives the equation

$$\frac{\partial f_{-1}}{\partial t} = \overline{S^{ioniz}} - \overline{\mathbf{v}_{Di} \cdot \nabla \psi} \frac{\partial f_{-1}}{\partial \psi} \quad (29)$$

The operator of *bounce averaging* is $\overline{A} = \frac{1}{T} \oint \frac{d\theta}{v_{\parallel} \hat{\mathbf{n}} \cdot \nabla \theta} A = \frac{1}{T} \int \frac{d\theta}{v_{\parallel}/(qR)} A$. The bounce time is $T = \oint \frac{d\theta}{v_{\parallel} \hat{\mathbf{n}} \cdot \nabla \theta} = \oint \frac{d\theta}{v_{\parallel}/(qR)}$. The limits of integrations for untrapped ions are $[-\pi, \pi]$ and for trapped ions the integral is defined

$$\oint d\theta = \sum_{\sigma} \sigma \int_{-\theta_0}^{+\theta_0} d\theta \quad (30)$$

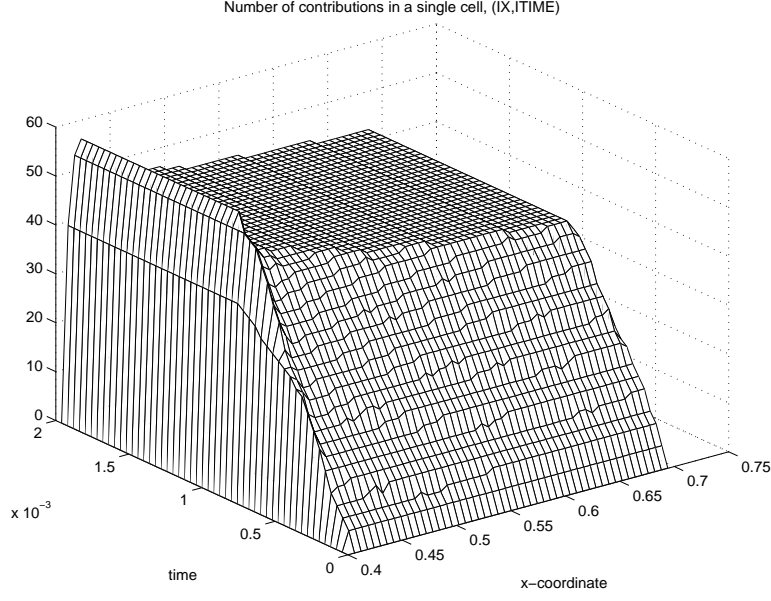


Figure 28: The (r, t) profile of the number of contributions that are registered in the cells of the mesh, coming from neighbor cells, as described in Figure 27.

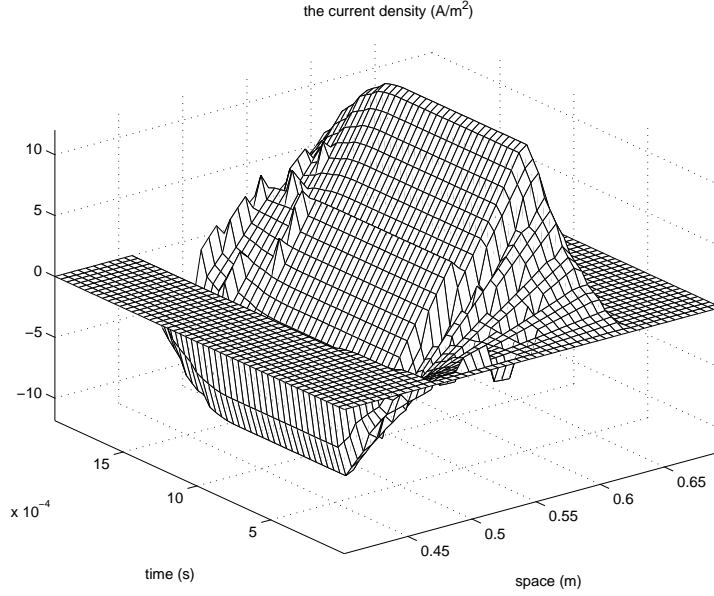


Figure 29: The (r, t) profile of the current density J (A/m^2).

where $-\theta_0$ and $+\theta_0$ are the *turning points* of the banana. The radial projection of the guiding centre drift velocity can be written

$$\mathbf{v}_{Di} \cdot \nabla \psi = I v_{\parallel} (\hat{\mathbf{n}} \cdot \nabla) \left(\frac{v_{\parallel}}{\Omega_{ci}} \right) = I v_{\parallel} \hat{\mathbf{n}} \cdot \nabla \theta \frac{\partial}{\partial \theta} \left(\frac{v_{\parallel}}{\Omega_{ci}} \right) \quad (31)$$

where $I = R^2 \mathbf{B} \cdot \nabla \varphi = R B_T \equiv I(\psi)$ is a function of only the magnetic surface variable (ψ) and $\hat{\mathbf{n}} \cdot \nabla \theta = 1/(qR)$. At this point we assume that the new ion has reached the asymptotic

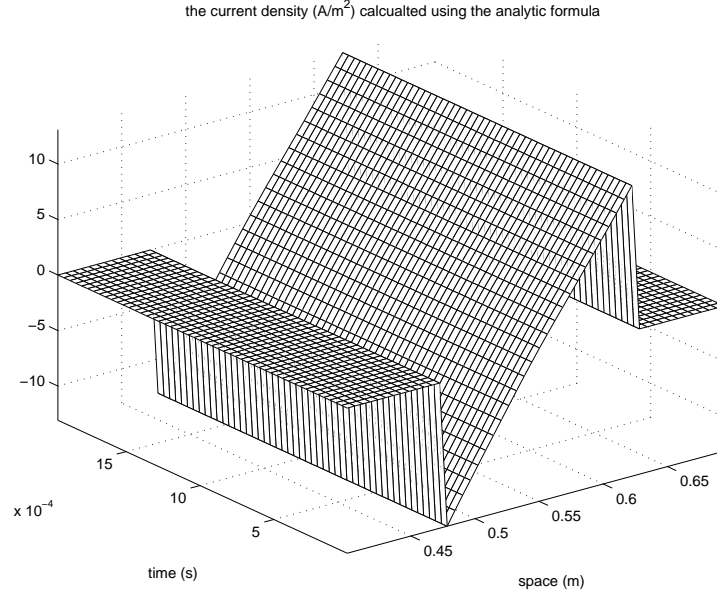


Figure 30: The first analytic formula that obtains the current density.

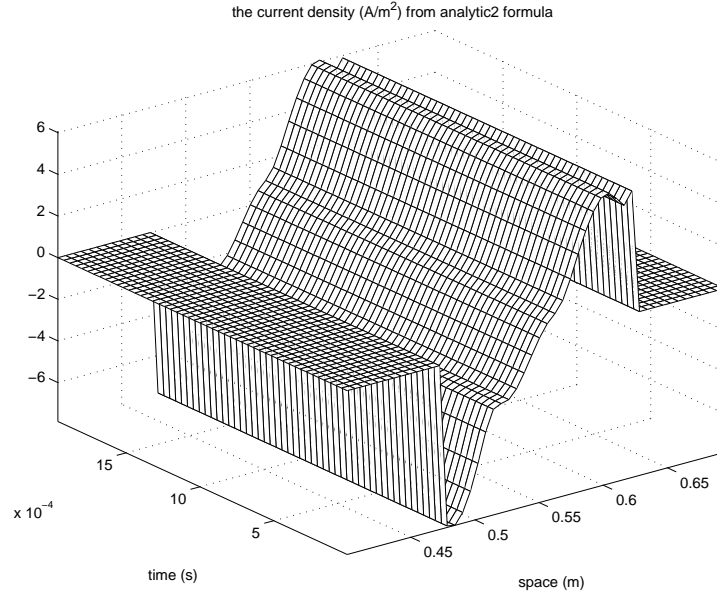


Figure 31: The second analytic formula for the current density.

periodic motion on the banana. Then the radial displacements average to zero

$$\overline{(\mathbf{v}_{Di} \cdot \nabla \psi)} = \frac{1}{T} \sum_{\sigma} \int_{-\theta_0}^{+\theta_0} \frac{d\theta}{v_{\parallel}/(qR)} I(\psi) \frac{v_{\parallel}}{qR} \frac{\partial}{\partial \theta} \left(\frac{v_{\parallel}}{\Omega_{ci}} \right) = 0 \quad (32)$$

Eq.(29) becomes

$$\frac{\partial f_{-1}}{\partial t} = \overline{S}^{ioniz} \quad (33)$$

and indeed f_{-1} appears as a direct result of the “external” source. The source of new ions

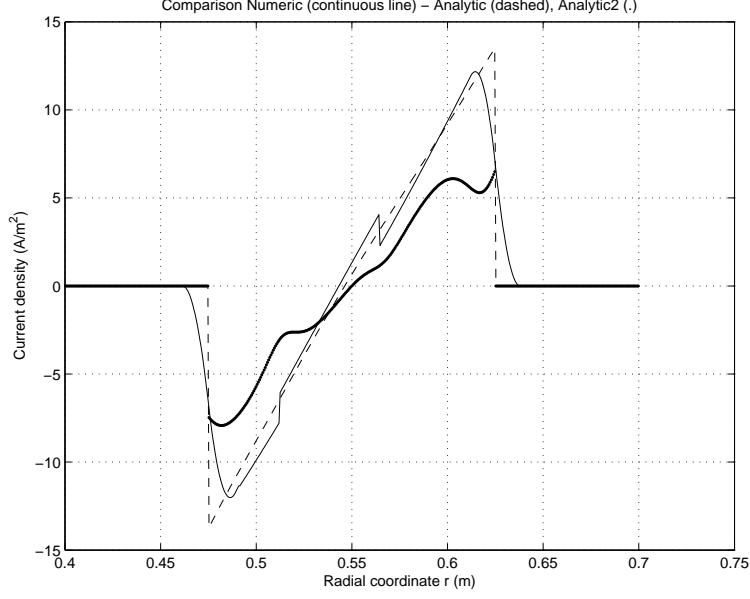


Figure 32: The comparison between the two analytic formulas and the result of the numerical calculation. The section is made at time that is half the total duration of the ionization process.

of velocity v_0 , with direction σ_0 and trapping parameter λ_0 is²³

$$\overline{S}^{ioniz} = \dot{n}^{ioniz}(\psi, t) \delta_{\sigma, \sigma_0} \Theta(t) \delta(\lambda - \lambda_0) \frac{\delta(v - v_0)}{\pi v_0^2} \quad (34)$$

The Eq.(33) simply describes the accumulation of new ions with $(v_0, \sigma_0, \lambda_0)$ on the surface ψ . The motion of these ions toward the banana trajectories and the periodic motion that follows must be found at higher orders. Returning to Eq.(28) we express f_0 in terms of f_{-1} , using (31)

$$v_{\parallel} \hat{\mathbf{n}} \cdot \nabla f_0 \equiv v_{\parallel} \nabla_{\parallel} f_0 = -v_{\parallel} \nabla_{\parallel} \left(\frac{I v_{\parallel}}{\Omega_{ci}} \right) \frac{\partial f_{-1}(\psi)}{\partial \psi} \quad (35)$$

with the solution

$$f_0(\psi, \theta, t) = -I \left(\frac{v_{\parallel}}{\Omega_{ci}} \right) \frac{\partial f_{-1}(\psi)}{\partial \psi} + g(\psi, \theta, t) \quad (36)$$

where a constant of integration of the operator ∇_{\parallel} is introduced. We make few remarks. First, the time dependence of f_0 inherited from f_{-1} will be essential for the presence in the theory of the first, transitory and unique, part of the trajectory. Further, the first term can be approximated, using for circular geometry $\frac{I}{B_T} \frac{\partial}{\partial \psi} \simeq \frac{1}{B_{\theta}} \frac{\partial}{\partial r}$,

$$-I \left(\frac{v_{\parallel}}{\Omega_{ci}} \right) \frac{\partial f_{-1}(\psi)}{\partial \psi} \approx -\frac{B}{B_{\theta}} \frac{v_{\parallel}}{\Omega_{ci}} \frac{\partial f_{-1}(r)}{\partial r} = -\frac{v_{\parallel}}{\Omega_{\theta ci}} \frac{\partial}{\partial r} f_{-1}(r) \quad (37)$$

and we see that the difference between the distribution function f_0 and that of the previous level (f_{-1}) consists of a radial shift of the space argument, of the order of the poloidal

Larmor radius $v_{\parallel}/\Omega_{\theta ci} \sim \rho_{\theta}$. This is the same relationship as between the first order neo-classical distribution function relative to the Maxwellian equilibrium distribution¹¹. In the particular case of trapped particles, the correction needs also to reflect the approximative relation between the thermal speed and the parallel velocity of ions²², and we have $v_{\parallel}/\Omega_{\theta ci} \approx (v_{th}/\Omega_{\theta ci})(r/R)^{1/2} = \rho_{\theta}\varepsilon^{1/2}$. Finally we note that g is constant on the magnetic lines, *i.e.* on surfaces, $\hat{\mathbf{n}} \cdot \nabla g = 0$. A distribution function for *bananas* can never be constant on the magnetic surfaces because the trajectory stops somewhere. Therefore g must only be added to (36) if we consider circulating particles. For our purpose it is not retained.

The next step is the equation for the *first order* f_1 , which is derived from the equation written at *zero-order*

$$\frac{\partial f_0}{\partial t} + v_{\parallel} \hat{\mathbf{n}} \cdot \nabla f_1 + \mathbf{v}_{Di} \cdot \nabla f_0 = 0 \quad (38)$$

This involves the variation of the first order correction function f_1 along the magnetic lines $v_{\parallel} \nabla_{\parallel} f_1 + \dots$

$$\mathbf{v}_{Di} \cdot \nabla f_0 = \mathbf{v}_{Di} \cdot \nabla \theta \frac{\partial f_0}{\partial \theta} + \mathbf{v}_{Di} \cdot \nabla \psi \frac{\partial f_0}{\partial \psi} \quad (39)$$

where $\mathbf{v}_{Di} = -v_{\parallel} \hat{\mathbf{n}} \times \nabla \left(\frac{v_{\parallel}}{\Omega_{ci}} \right)$.

$$\mathbf{v}_{Di} \cdot \nabla \theta = v_{\parallel} \frac{1}{r} R B_{\theta} \frac{\partial}{\partial \psi} \left(\frac{v_{\parallel}}{\Omega_{ci}} \right) \quad (40)$$

and similarly

$$\mathbf{v}_{Di} \cdot \nabla \psi = -\frac{v_{\parallel}}{r} R B_{\theta} \frac{\partial}{\partial \theta} \left(\frac{v_{\parallel}}{\Omega_{ci}} \right) \quad (41)$$

Returning to the initial expression

$$\mathbf{v}_{Di} \cdot \nabla f_0 = I \frac{v_{\parallel}}{qR} \left[\frac{\partial}{\partial \psi} \left(\frac{v_{\parallel}}{\Omega_{ci}} \right) \frac{\partial f_0}{\partial \theta} - \frac{\partial}{\partial \theta} \left(\frac{v_{\parallel}}{\Omega_{ci}} \right) \frac{\partial f_0}{\partial \psi} \right] \quad (42)$$

The *bounce average* is

$$\overline{(\mathbf{v}_{Di} \cdot \nabla f_0)} = \frac{1}{T} I \int_{-\theta_0}^{+\theta_0} \frac{d\theta}{v_{\parallel}/(qR)} \frac{v_{\parallel}}{qR} \left[\frac{\partial}{\partial \psi} \left(\frac{v_{\parallel}}{\Omega_{ci}} \right) \frac{\partial f_0}{\partial \theta} - \frac{\partial}{\partial \theta} \left(\frac{v_{\parallel}}{\Omega_{ci}} \right) \frac{\partial f_0}{\partial \psi} \right] \quad (43)$$

Here we replace f_0 with its expression in terms of f_{-1} ;

$$f_0(\psi, \theta, t) = -I \left(\frac{v_{\parallel}}{\Omega_{ci}} \right) \frac{\partial f_{-1}(\psi)}{\partial \psi} \quad (44)$$

$$\begin{aligned}
& \overline{(\mathbf{v}_{Di} \cdot \nabla f_0)} \\
&= -\frac{I^2}{T} \int_{-\theta_0}^{+\theta_0} d\theta \left\{ \frac{\partial}{\partial \psi} \left(\frac{v_{\parallel}}{\Omega_{ci}} \right) \frac{\partial}{\partial \theta} \left(\frac{v_{\parallel}}{\Omega_{ci}} \right) \frac{\partial f_{-1}(\psi)}{\partial \psi} + \frac{\partial}{\partial \psi} \left(\frac{v_{\parallel}}{\Omega_{ci}} \right) \left(\frac{v_{\parallel}}{\Omega_{ci}} \right) \frac{\partial^2 f_{-1}(\psi)}{\partial \theta \partial \psi} \right. \\
&\quad \left. - \frac{\partial}{\partial \theta} \left(\frac{v_{\parallel}}{\Omega_{ci}} \right) \frac{\partial}{\partial \psi} \left(\frac{v_{\parallel}}{\Omega_{ci}} \right) \frac{\partial f_{-1}(\psi)}{\partial \psi} - \frac{\partial}{\partial \theta} \left(\frac{v_{\parallel}}{\Omega_{ci}} \right) \left(\frac{v_{\parallel}}{\Omega_{ci}} \right) \frac{\partial^2 f_{-1}}{\partial \psi^2} \right\}
\end{aligned} \tag{45}$$

The first and third terms cancel. In addition we know from (27) that f_{-1} is constant on the magnetic surfaces. *i.e.* the second term is zero. It remains

$$\overline{(\mathbf{v}_{Di} \cdot \nabla f_0)} = \frac{I^2}{T} \frac{\partial^2 f_{-1}}{\partial \psi^2} \int_{-\theta_0}^{+\theta_0} d\theta \frac{\partial}{\partial \theta} \left[\frac{1}{2} \left(\frac{v_{\parallel}}{\Omega_{ci}} \right)^2 \right] = 0 \tag{46}$$

We can now calculate the radial current, using the distribution functions in orders -1 , 0 , 1 . This is obtained from the radial projection of the drift velocity, Eq.(31)

$$\mathbf{v}_{Di} \cdot \nabla \psi = I \frac{v_{\parallel}}{qR} \frac{\partial}{\partial \theta} \left(\frac{v_{\parallel}}{\Omega_{ci}} \right) \tag{47}$$

The current is projected on the radial direction and the result is averaged over the magnetic surface, with the operator $\langle A \rangle = w^{-1} \int A r d\theta / B_{\theta}$, $w = \int r d\theta / B_{\theta}$,

$$\langle \mathbf{j} \cdot \nabla \psi \rangle = |e| \left\langle \int d^3v (\mathbf{v}_{Di} \cdot \nabla \psi) f \right\rangle = -|e| I \left\langle \int d^3v \left(\frac{v_{\parallel}}{\Omega_{ci}} \right) v_{\parallel} \hat{\mathbf{n}} \cdot \nabla f \right\rangle \tag{48}$$

An integration by parts over θ has been done. Two terms are absent: (1) the order -1 distribution function f_{-1} does not contribute due to (27); and (2) the order 0 does not contribute, due to (46). The first order to have a contribution to this current (averaged over surface) is f_1 . From the equation (38) we take the term

$$v_{\parallel} \hat{\mathbf{n}} \cdot \nabla f_1 = -\frac{\partial f_0}{\partial t} - \mathbf{v}_{Di} \cdot \nabla f_0 \tag{49}$$

and Eq.(48) becomes

$$\langle \mathbf{j} \cdot \nabla \psi \rangle = -|e| I \left\langle \int d^3v \left(\frac{v_{\parallel}}{\Omega_{ci}} \right) \left(-\frac{\partial f_0}{\partial t} - \mathbf{v}_{Di} \cdot \nabla f_0 \right) \right\rangle \tag{50}$$

The surface average operator applied on the second term in the bracket vanishes

$$\left\langle \int d^3v \left(\frac{v_{\parallel}}{\Omega_{ci}} \right) (\mathbf{v}_{Di} \cdot \nabla f_0) \right\rangle = 0 \tag{51}$$

This is shown by a calculation analogous to that of Eq.(39), using (40) and (41) followed by the substitution of (44). The current is

$$\langle \mathbf{j} \cdot \nabla \psi \rangle = |e| I \left\langle \int d^3v \left(\frac{v_{\parallel}}{\Omega_{ci}} \right) \frac{\partial f_0}{\partial t} \right\rangle \tag{52}$$

We use the zero-order function f_0 from Eq.(44) and take the time derivative,

$$\langle \mathbf{j} \cdot \nabla \psi \rangle = -|e| I^2 \left\langle \int d^3v \left(\frac{v_{\parallel}}{\Omega_{ci}} \right)^2 \frac{\partial^2 f_{-1}}{\partial \psi \partial t} \right\rangle \quad (53)$$

where, in (34) we keep the isotropic velocity space integration $d^3v = 4\pi v^2 dv$ and introduce the factorization (2)

$$\frac{\partial f_{-1}}{\partial t} = \bar{S}^{ioniz} = \dot{n}_0^{ioniz} S(r, t) \frac{1}{4\pi v^2} \delta(v - v_0) \quad (54)$$

For circular surfaces

$$\langle j_r \rangle \approx -|e| \frac{B_T^2}{B_\theta^2} \left\langle \int d^3v \left(\frac{v_{\parallel}}{\Omega_{ci}} \right)^2 \frac{\partial^2 f_{-1}}{\partial r \partial t} \right\rangle \quad (55)$$

We note again the presence of the poloidal gyroradius, corrected for trapped particles ($v_{\parallel} = (r/R)^{1/2} v_{th}$),

$$\frac{B_T^2}{B_\theta^2} \left(\frac{v_{\parallel}}{\Omega_{ci}} \right)^2 \approx \left(\frac{v_{\parallel}}{\Omega_{\theta ci}} \right)^2 = \rho_\theta^2 \varepsilon = \rho_i^2 q^2 \varepsilon^{-1} \quad (56)$$

This length ($\rho_\theta \varepsilon^{1/2}$) corresponds to the radial excursion of the new ion, as defined in our previous approach, Eq.(21)

$$\rho_\theta \varepsilon^{1/2} = \rho_i q \varepsilon^{-1/2} \approx \Delta^{t\pm} \quad (57)$$

After replacing the expression of $\partial f_{-1}/\partial t$ Eq.(54) we have

$$\begin{aligned} \langle j_r \rangle &= -|e| \left\langle \int d^3v \rho_\theta^2 \varepsilon \frac{\partial}{\partial r} \dot{n}_0^{ioniz} S(r, t) \frac{1}{4\pi v^2} \delta(v - v_0) \right\rangle \\ &= -|e| \dot{n}_0^{ioniz} \frac{\partial S(r, t)}{\partial r} \langle \rho_\theta^2 \varepsilon \rangle = -|e| \dot{n}_0^{ioniz} \frac{\partial S(r, t)}{\partial r} \langle (\Delta^{t\pm})^2 \rangle \end{aligned} \quad (58)$$

It is understood that ρ_θ and further $\Delta^{t\pm} = \rho_i q \varepsilon^{-1/2}$ are calculated at the velocity v_0 . As before we replace the λ -integration with multiplication with $\sqrt{\varepsilon}$, fraction of trapped particles

$$j_r = -\gamma |e| \dot{n}_0^{ioniz} \frac{\partial S(r, t)}{\partial r} \rho_i^2 q^2 \varepsilon^{-1/2} \quad (59)$$

The constant γ is a purely neoclassical constant and is calculated, for more general conditions, in²³. It includes the exact integration over the trapping parameter λ , which is contained in v_{\parallel} at v_0 fixed. The result is $\gamma \sim 0.38$.

We note that the analytic structure of our result Eq.(22) and of its rederivation in the neoclassical drift-kinetic theory, Eq.(59) are the same as the expression obtained in the treatment of Rosenbluth and Hinton for the current induced by the α particles²³. The coefficient in our approximate treatment Eq.(22) is $\gamma \sim 1/2$. Figure 5 represents the space

dependence of the current $J(r, t_0)$ obtained from the analysis of the physical picture, Eq.(20), from the numerical model and respectively from Eq.(22) which is also the result of the drift-kinetic approach. The time t_0 is chosen at half the total time interval, to avoid the transient after the onset of ionization.

We note that the conclusion of the mentioned paper, that the rotation induced by the creation of *alpha* particles is insignificant is a consequence of the very small nuclear reaction rate. The equivalent parameter, in the present problem, is the rate of generation of new ions, which is three orders of magnitude higher in the case of pellets.

The two treatments (the simple arguments related with the fluxes of ions and, respectively, the drift-kinetic equation) lead to the same result but there is an apparent difference between them. In the first treatment the separation of the trajectory of a new ion in a transitory part, where effective current exist, and a periodic part with no effective radial current is the key element that identifies the source of current, torque, rotation. In the drift-kinetic approach this separation is not obvious. One would expect an “initial value problem” where the distribution function would result as integral over the history of the ion’s motion. This is not visible. The Heaviside function of the source is not helpful either: it marks the beginning of the ionization process but after that every moment of time is a source of new ions and this is not represented. We understand however that the separation is implicitly done through the velocity space integration. The current is defined as $j \sim |e| \langle v_{Di} \int d^3v \bar{f}(r, v) \rangle$. The late phase of the ion orbit is periodic and the integral mixes to zero the two-way travels on banana, leaving only the first, non-periodic, part.

V. DISCUSSION AND CONCLUSION

The gas puff, the pellets, the impurity seeding and in general any inflow of neutrals into plasma produce a substantial radial current and implicitly a torque that can be higher than the magnetic pumping damping. It can be shown that it can also be higher than the turbulent Reynolds stress and the Stringer mechanism. We have derived a simple analytical expression which is confirmed by numerical simulation. Furthermore, we have re-derived it within the neoclassical drift-kinetic approach. All three methods have close quantitative results, as shown in Figure 5. We mention, qualitatively, few possible consequences.

PEP regimes²⁴ seem to be connected with the ionization-induced rotation that improves

the local confinement by creating effective barriers through the sheared poloidal flow⁶. The duration of the PEP and the density peaking are compatible with ionization-induced rotation.

The ionization-induced radial current leads to density peaking, in at least three different ways. If the gradient of the rate of ionization of a pellet is negative ($\partial S/\partial r < 0$, higher ionization rate close to the plasma center, as for pellets launched from high-field side) then the current Eq.(22) is directed toward the edge. The bulk ions must move toward the magnetic axis to compensate this current. Schematically, we consider a new ion that moves a distance Δ toward the edge and then “stops” (actually it moves periodically on banana). An ion of the background must move in opposite direction the same distance Δ . But in that moment another new ion is created at a distance Δ from this position, closer to the center and starts moving toward the edge. Then the background ion must continue its displacement toward the center to compensate this new current. While any new ion move a distance Δ then stops, the background ion must continue to move to compensate the small currents. Quantitatively the two fluxes are balanced but ions from edge can travel very far toward the center. Impurity accumulation in the center can also be produced in this process.

Second, the rotation produced at ionization is necessarily sheared, *i.e.* $v_\theta = v_\theta(r)$, for two reasons. In the regions of positive and respectively negative radial derivative of the rate of ionization ($\partial S/\partial r \gtrless 0$) the rotation has opposite direction (Figures 3 and 5). In addition, the background ions must have a local rotation that is opposite to that of the new ions. The rate of extraction of the free energy from density gradients is reduced and the turbulence will have shorter radial correlation length. The rate of transport decreases and the peaking of the density in the center is enhanced by the smaller density diffusion.

Third, the shear of the poloidal velocity is actually vorticity $\omega = \partial v_\theta/\partial r$ and when this occurs the Ertel’s theorem $\frac{d}{dt} \left(\frac{\omega + \Omega_{ci}}{n} \right) = 0$ imposes a redistribution of density.

A change of the density at the edge, by impurity seeding¹⁵ or by other strong ionization event, must now also be regarded as an electric process, due to the charge separation and the radial current of the new ions. It implies that very fast plasma responses should be expected²⁵. This may explain observed fast propagation of perturbations, sometimes called “non-local”. Fast increase of the radial electric field is able to determine, as a neoclassical effect, the reversal of the toroidal rotation^{21, 20, 26}.

In conclusion, we have presented arguments that the neoclassical displacements of the new ions generated at ionization (of gas puff, pellet, impurity seeding) produce a radial current that can be substantial. The current is generated from the first part, transitory, unique for any ionization event, of the trajectory: between the ionization and the moment where the new ion reaches the stationary periodic motion, trapped or circulating. The torque resulting from ionization can be substantial and it can generate internal transport barriers. Our perspective on some particular regimes may need reconsideration: Pellet Enhanced Performance, density peaking, density pinch, regimes with density higher than the Greenwald limit, fast propagation of edge effects, influence of the density on the transition to H -mode, connection between density and rotation, reversal of toroidal rotation, etc. A more detailed investigation of the ionization-induced rotation is requested, for each of these cases.

A. APPENDIX. COMPARISON OF THE CURRENTS CARRIED BY TRAPPED AND RESPECTIVELY CIRCULATING IONS

The equation of the closed orbit (poloidal projection of the orbit of a circulating ion) is

$$(x + \alpha r_0)^2 + y^2 = r_0^2 \quad (\text{A.1})$$

a circle of radius r_0 that is displaced from the magnetic axis with the amount $x_0 = \alpha r_0$ where $\alpha = (B/B_T) v_{Di}/v_{\parallel} = \text{const.}$ ¹⁸. We have $\alpha \ll 1$ (since $v_{Di} \ll v_{\parallel} \sim v_{th,i}$) for circulating ions. Therefore the radial displacement of the “center” of the orbit of a new ion that is circulating, relative to the center of the magnetic surface where it is created, is small. The displacement x_0 of circulating ions that are created closer to the edge (at higher r_0) are larger than that created closer to the magnetic axis. For two ions born in the same point on the equatorial plane and with velocities parallel respectively anti-parallel to \mathbf{B} the difference between these displacements is linear in r ,

$$\begin{aligned} |x_0^{(+)} - x_0^{(-)}| &= \left| \left(x_{0c} + \alpha \frac{\partial r_0}{\partial r} x_0^{(+)} \right) - \left(x_{0c} - \alpha \frac{\partial r_0}{\partial r} x_0^{(-)} \right) \right| \\ &= \alpha \frac{\partial r_0}{\partial r} (x_0^{(+)} + x_0^{(-)}) = 2\alpha^2 r_0 \end{aligned} \quad (\text{A.2})$$

This is indeed very small, due to α^2 factor. The closed orbit for parallel initial velocity, (+), is fully contained inside the magnetic surface, which means that the displacement $x_0^{(+)}$

is positive. The closed orbit for the anti-parallel initial velocity, $(-)$, fully encloses the magnetic surface, which means that the displacement $x_0^{(-)}$ is negative. In absolute value $x_0^{(+)}$ is greater than $x_0^{(-)}$. Note that we here use the geometric “center of the closed orbit” and *not* the asymptotic value of the average $\bar{x}(t \rightarrow \infty)$. The latter are closer the main axis of symmetry, for both sign of the initial velocities.

The current carried by the new ions for the short time until they access the stationary periodic motion relies on the difference between the displacements $n^c \left| x_0^{(+)} - x_0^{(-)} \right| = n^c 2\alpha^2 r$ is directed towards the main axis of the torus. The ratio between the width of the banana and the displacement of the center for a circulating particle originating from the same point is approximately¹⁸

$$\frac{\Delta^\pm}{x_0^{(\pm)}} = 4\sqrt{\frac{R_0}{r}} \quad (\text{A.3})$$

The second term in Eq.(20) is in general greater than the first. We then compare the current from circulating ions with only this first term. We find that the circulating ions’ contribution is smaller than this term, which justifies their neglect adopted in the main text. We have to compare the charge displacements, including the densities of trapped (n^t) and circulating (n^c) particles. We expand, taking as reference position the point r where the two ions (with parallel and anti-parallel \mathbf{v}_0) are born, $\Delta^{(+)} - \Delta^{(-)} = \frac{\partial \Delta}{\partial r} [\Delta^{(+)} + \Delta^{(-)}]$. In the right hand side, and in all expressions where the difference between Δ^\pm is not involved, we can approximate $\Delta = \Delta^\pm(r) \approx \rho_i q(r) \varepsilon^{-1/2}/2$.

$$\frac{n^t |\Delta^{(+)} - \Delta^{(-)}|}{n^c |x_0^{(+)} - x_0^{(-)}|} \approx \frac{\frac{1}{2} n^t \frac{(\rho_i q)^2}{\varepsilon} \frac{\partial}{\partial r} \ln(qr^{-1/2})}{2n^c \alpha^2 r} \quad (\text{A.4})$$

We use $\partial \varepsilon / \partial r \approx 1/R$ and $(\rho_i q) = 2\Delta\sqrt{\varepsilon}$ obtaining the ratio

$$\frac{1}{\alpha^2 r^2} R (\rho_i q)^2 = r \left(\frac{\Delta}{x_0} \right)^2 \quad (\text{A.5})$$

Then

$$\frac{n_i^t |\Delta^{(+)} - \Delta^{(-)}|}{n_i^c |x_0^{(+)} - x_0^{(-)}|} = \frac{n_i^t}{n_i^c} r \left(\frac{\Delta}{x_0} \right)^2 \frac{1}{4} \frac{\partial}{\partial r} \ln(qr^{-1/2}) \quad (\text{A.6})$$

The ratio of the densities of trapped and circulating particles is

$$\frac{n_i^t}{n_i^c} \approx \frac{\sqrt{\varepsilon}}{1 - \sqrt{\varepsilon}} \quad (\text{A.7})$$

and employing Eq.(A.3)

Then

$$\frac{n^t |\Delta^{(+)} - \Delta^{(-)}|}{n^c |x_0^{(+)} - x_0^{(-)}|} \approx 4R_0 \frac{\sqrt{\varepsilon}}{1 - \sqrt{\varepsilon}} \frac{\partial}{\partial r} \ln(qr^{-1/2}) \quad (\text{A.8})$$

In the region of interest $[r_1, r_2]$ it is sufficient to approximate $q \sim 1 + \beta (r/a)^2$ with β a constant. Retaining the dominant term, $\frac{\partial}{\partial r} \ln(qr^{-1/2}) \sim \frac{3}{2} \frac{1}{r}$ we have the estimation

$$\frac{n^t |\Delta^{(+)} - \Delta^{(-)}|}{n^c |x_0^{(+)} - x_0^{(-)}|} \approx \frac{6}{\sqrt{\varepsilon} - \varepsilon} \gg 1 \quad (\text{A.9})$$

This justifies the neglect of the current from the circulating ions in Eqs.(19) and (20).

B. APPENDIX. THE MOMENTUM OF THE PLASMA ROTATION INDUCED BY IONIZATION

As mentioned in Section III in the present case the total torque is zero and there is no problem of conservation of the angular momentum. For more general $S(x, t)$ the source of angular momentum and energy related to the “spontaneous rotation” requires a discussion, which we here attempt in general terms.

Assume a *slab-like* geometry with the plasma immersed in a static magnetic field $\mathbf{B} = B\hat{\mathbf{e}}_z$. From external sources it is applied a transversal electric field $\mathbf{E} = E\hat{\mathbf{e}}_x$ field. There is a motion of the plasma in the direction $\hat{\mathbf{e}}_y$ with the speed $\mathbf{v}_E = \mathbf{E} \times \mathbf{B}/B^2$, which apparently violates the conservation of the momentum along the y direction: before applying \mathbf{E} there was no momentum along y but after that we find plasma moving along y with all its particles.

There is, of course, no “spontaneous generation of momentum”. The momentum that would ensure the conservation and which seems to be missing is actually taken over by the external fields \mathbf{B} and \mathbf{E} . They are acting as an intermediate medium transferring the momentum of the guiding center $m_i \mathbf{v}_E$ to the external structure (in general coils and condensers) that maintains these fields.

We consider charges of density $\rho(\mathbf{r}, t)$ and currents of density $\mathbf{j}(\mathbf{r}, t)$ in a limited volume V bounded by the surface Σ . From the Maxwell equation one derives the local balance

$$\nabla \cdot \mathcal{S} = \rho \mathbf{E} + \mathbf{j} \times \mathbf{B} + \varepsilon_0 \frac{\partial}{\partial t} (\mathbf{E} \times \mathbf{B}) \quad (\text{B.1})$$

with $\mathcal{S} = \mathcal{S}^{(e)} + \mathcal{S}^{(m)}$, where the components of the order-two tensor $\mathcal{S}^{(e)}$ are²⁸

$$(\mathcal{S}^{(e)})_{ij} = \varepsilon_0 E_i E_j - \varepsilon_0 \frac{1}{2} \delta_{ij} E^2 \quad (\text{B.2})$$

and respectively

$$(\mathcal{S}^{(m)})_{ij} = \frac{1}{\mu_0} B_i B_j - \frac{1}{\mu_0} \frac{1}{2} \delta_{ij} B^2 \quad (\text{B.3})$$

For a point-like particle of charge $|e|$ with trajectory $\mathbf{r}_0(t)$,

$$\begin{aligned} \rho(\mathbf{r}, t) &= |e| \delta^3[\mathbf{r} - \mathbf{r}_0(t)] \quad (C/m^3) \\ \mathbf{j}(\mathbf{r}, t) &= |e| \mathbf{v} \delta^3[\mathbf{r} - \mathbf{r}_0(t)] \quad (A/m^2) \end{aligned} \quad (\text{B.4})$$

Eq.(B.1) is integrated over the volume V

$$\int_{\Sigma} \mathcal{S} \cdot \hat{\mathbf{n}} \, da = \mathbf{F}^{(e)} + \mathbf{F}^{(m)} + \varepsilon_0 \frac{\partial}{\partial t} \int_V dv (\mathbf{E} \times \mathbf{B}) \quad (\text{B.5})$$

where one notes that the quantity $\varepsilon_0 \mathbf{E} \times \mathbf{B}$ is a volume density of momentum and the last term

$$\mathbf{P}^{em} \equiv \varepsilon_0 \int_V dv (\mathbf{E} \times \mathbf{B}) \quad (\text{B.6})$$

represents the amount of *momentum of the electromagnetic field* inside the volume V . This underlies the role of the tensor \mathcal{S} : the quantity $\mathcal{S} \cdot \hat{\mathbf{n}}$ is the flux of momentum through the element of area da of the surface Σ . The total mechanical force acting on the particles and currents can be expressed as the time derivative of the *mechanical momentum* inside V

$$\mathbf{F}^{(e)} + \mathbf{F}^{(m)} = \frac{d}{dt} \mathbf{P}^{mech} \quad (\text{B.7})$$

Then the equation becomes

$$\int_{\Sigma} \mathcal{S} \cdot \hat{\mathbf{n}} \, da = \frac{d}{dt} (\mathbf{P}^{mech} + \mathbf{P}^{em}) \quad (\text{B.8})$$

Anything that changes inside V (field, motion) must be balanced by a reaction from the world exterior to V . Now we imagine that Σ is very large, enclosing the toroidal coils, etc. such that the fields have vanished on the boundary. Then

$$\frac{d}{dt} \mathbf{P}^{mech} = - \frac{d}{dt} \mathbf{P}^{em} \quad (\text{B.9})$$

which expresses in the most clear way the idea of this discussion: any modification of the mechanical momentum of the charged particle must be balanced by an opposite modification of the electromagnetic field. For externally applied (\mathbf{B}, \mathbf{E}) fields, the momentum (and angular momentum) is sustained by a reaction against the sources of the fields, coils and condensers.

When the electric field is generated by charge separation inside plasma, the momentum and the energy of the guiding centers will necessarily involve the momentum and energy inside plasma, besides those external to it. After ionization, the new ions take energy by interacting with the background plasma and it is with this energy that they move to settle on final periodic orbits. Their motion produces the layer of unbalanced ion charge at the edge of the ionization region and the resulting electric (E^I) field is fully dependent on the energy of the new ions. Then the momentum and energy of the plasma moving with $\mathbf{v}_E = \mathbf{E}^I \times \mathbf{B} / B^2$ have their origin in the energy that the new ions could get from the background plasma. The rotation \mathbf{v}_E is a backreaction, like an inertia. The plasma responds to E^I by polarization drift of the background ions. Moving on a distance $\delta x^L = (\Omega_{ci} B)^{-1} E^I$ in the field E^I the variation in energy is $\delta W = n^{bg} |e| E^I \times (\Omega_{ci} B)^{-1} E^I = \delta \left(n^{bg} \frac{m_i v_E^2}{2} \right)$ which is the variation in energy of the rotation of the plasma. We can see that the plasma rotation v_E is significant only if the background plasma feeds the new ions with sufficient energy for them to reach trapping orbits with substantial $\Delta^{t\pm}$ *i.e.* such that the charge separation produces a large \mathbf{E}^I .

C. APPENDIX. PLASMA RESPONSE TO THE CHARGE SEPARATION INDUCED BY THE DISPLACEMENT OF THE NEW IONS

After ionization the new ions move to take their neoclassical periodic orbit. Between the point of creation and the “center” of the periodic motion they carry a transitory, short, finite current. As in the main text we consider the ionization to take place in a volume limited between the radii r_1 (left side, closer to the center) r_2 (right side, closer to the last closed magnetic surface). The plasma is considered homogeneous and the ionization generates ions that move to the right a distance Δ^t with velocity v_{Di} while the new electrons can be considered immobile. Then most of the volume between r_1 and r_2 is neutral but at the right end $\sim r_2$ of the ionization interval it results a layer (denoted I) of positive charge, of width Δ^t . This is the source of electric field, resulted from ionization, E^I , directed from r_2 towards r_1 . The charge layer I and its field E^I are built up on a time scale $\delta t = \Delta^t / v_{Di}$ in which $\partial E^I / \partial t > 0$. The background plasma responds by modifying the Larmor gyration orbit from the usual circle to a cycloid (actually the new orbit is a *prolate trochoid*). The deformation of the gyration directly indicates the expected $\mathbf{v}_E = \mathbf{E} \times \mathbf{B} / B^2$ motion and

also the asymmetry of the charge distribution along the new orbit. The asymmetry creates a new layer (denoted L) of positive (ion) charge, at the left end, $\sim r_1$ and an electric field E^L opposite to E^I . This field is sufficient to almost cancel E^I inside plasma, leaving in the interior a small $E^{int} = E^I - E^L$, directed to the left, like E^I . The asymmetry of the modified Larmor orbit is a manifestation of the polarization drift induced by the variation in time of the electric field E^I (implicitly E^{ind}), a displacement of the background ions in the direction to which points E^I (*i.e.* to the left). Since the ionization continues to accumulate new ions in the layer I , hence $\partial E^I / \partial t > 0$, the ion's drift of polarization $v_{Di}^{(pol)}$ fills the layer L at the left end, whose electric field E^L (from r_1 toward r_2) continues to quasi-compensate E^I inside plasma.

Qualitatively, this picture conforms to the concept of *return current*, which is universally invoked as the plasma response to any mechanism that is able to produce rotation of only some component of the density: NBI, ICRH, *alpha* particle, etc., to which we add: ionization. In the following we examine the density of charge and respectively the current density arising from ionization, deformation of the Larmor orbit and finally the polarization drift. The ionization-induced charge separation and current are regarded as “external” factors since they are requested by the geometry of the field.

We first include a justification of the neglect of the volume-charge accumulation that can be associated with the strong vorticity.

A. Charge and current related to the vorticity

At the edge of the tokamak in the H -mode regime there is a layer of strong poloidal rotation, with radial extension of about a banana width calculated for the poloidal magnetic field. The variation of the velocity magnitude is very fast in this layer, or, equivalently, the layer is a concentration of vorticity $\omega = \nabla \times \mathbf{v}$ or $\omega \sim \frac{\partial v_\theta}{\partial r}$. Taking as usual $\mathbf{v} = \mathbf{v}_E = \frac{-\nabla\phi \times \hat{\mathbf{e}}_z}{B}$ we have $\omega = \nabla \times \mathbf{v} = -\frac{\nabla^2 \phi}{B} \hat{\mathbf{e}}_z$ or

$$\omega = -\nabla^2 \phi / B \quad (\text{C.1})$$

directed along the magnetic field line. The Laplacian of the electric potential $\Delta\phi$ is the electric charge density and we have the well known situation that a vorticity is formally equivalent to a density of electric charge. If this charge is quantitatively important, it must

be taken into account together with the currents

$$\frac{\partial \rho^V}{\partial t} + \nabla \cdot \mathbf{J} = 0 \quad (\text{C.2})$$

where the “charge” $\nabla^2 \phi = -\rho^V / \varepsilon_0$ is the *vorticity*

$$\rho^V = -\varepsilon_0 \omega B \quad (\text{C.3})$$

We can estimate the magnitude of the charge density ρ^V . If the poloidal velocity has a spatial variation from $v_\theta = 0$ at the edge of the rotation layer and reaches amplitude of ~ 10 (km/s) on a radial extension of 10^{-2} (m) then $\omega \sim 10^7$ (s⁻¹) and this means

$$\rho^V \approx 3 \times 10^{-4} \text{ (C/m}^3\text{)} \quad (\text{C.4})$$

If the formation of this vorticity layer takes place on an interval controlled by the drift of the ions then

$$\delta t \sim \frac{\delta r}{v_{Di}} = \frac{10^{-2} \text{ (m)}}{30 \text{ (m/s)}} = 3 \times 10^{-4} \text{ (s)} \quad (\text{C.5})$$

and the time variation of the charge is

$$\frac{\partial \rho^V}{\partial t} \sim \frac{\rho^V}{\delta t} = \frac{3 \times 10^{-4} \text{ (C/m}^3\text{)}}{3 \times 10^{-4} \text{ (s)}} = 1 \left(\frac{\text{A}}{\text{m}^3} \right) \quad (\text{C.6})$$

This must be compared with $\nabla \cdot \mathbf{J}^I$. Taking the value estimated in the text $J^I \sim 10$ (A/m²) and a spatial variation on the same radial extension $\delta r \sim 10^{-2}$ (m) we have $\|\nabla \cdot \mathbf{J}^I\| \sim 10^3$ (A/m³). This is much higher than the time derivative of the vorticity-charge, so we can neglect this latter component of the physical picture. We must remember however that $J^I \sim 10$ (A/m²) is obtained for pellets while in other cases (*e.g.* neutrals penetrating from the edge) can be orders of magnitude smaller. In addition the interaction between ions and neutrals in this region is complex⁸. Then we have to check the possibility to neglect the vorticity-charge.

B. The charge accumulation and the current induced by ionization

The rate of increase of the density of charge ρ^I by influx of the new ions in the region of unbalanced charge at the right end $\sim r_2$ of the segment of ionization (the charge layer I) is $d\rho^I/dt \sim |e| \dot{n}_{ioniz} [\Theta(r - r_2) \Theta(r_2 + \Delta^t - r)]$ (C/m³/s), where Θ is the Heaviside function.

The width of the layer I is Δ^t and the time scale to fill with newly born ions is $\delta t \sim \Delta^t/v_{Di}$. Using the Gauss law

$$\frac{\partial E^I}{\partial x} = \frac{1}{\varepsilon_0} \rho^I \quad (\text{C.7})$$

we take the time derivation and integrate over x (actually $x \equiv r$ and we use x instead of r to underline the 1D geometry assumed here),

$$\frac{\partial E^I}{\partial t} = \Delta^t \frac{1}{\varepsilon_0} |e| \dot{n}_{ioniz} \left(\frac{V}{ms} \right) \quad (\text{C.8})$$

According to the source of ionization (neutrals penetrating from the edge, pellets, etc.) $\|\partial E^I/\partial t\|$ can vary over an interval of three orders of magnitude $\sim 10^9 \dots 10^{12} \left(\frac{V}{ms} \right)$. The static magnitude of E^I can be obtained from the surface charge density $\sigma^I = \rho^I \Delta^t$, as $E^I = \sigma^I/\varepsilon_0$.

The current density induced by ionization is calculated in the main text

$$J^I(r) \approx -\frac{1}{2} |e| \dot{n}_0^{ioniz} \left(\frac{\partial S}{\partial r} \right) \rho_i^2 q^2 \varepsilon^{-1/2} \quad (\text{C.9})$$

However this calculation was adapted to a particular class of cases and it must be reconsidered for other cases. We just mention the order of magnitude $J^I(x_C, t) \approx 10 \text{ [A/m}^2\text{]}$.

C. The charge accumulation and the current produced by the ion's drift of polarization

An ion in a constant magnetic field $\mathbf{B} = \hat{\mathbf{e}}_z B$ performs the Larmor gyration in the transversal plane xOy , on a circle of radius ρ_i with frequency $\Omega_{ci} = |e| B/m_i$. When a constant electric field $\mathbf{E} = \hat{\mathbf{e}}_x E$ is added, the circle is deformed into a curve of the cycloid type. Integrating the equation

$$\frac{d^2 \mathbf{r}}{dt^2} = \frac{|e| E}{m_i} \hat{\mathbf{e}}_x + \frac{|e| B}{m_i} \frac{d\mathbf{r}}{dt} \times \hat{\mathbf{e}}_z \quad (\text{C.10})$$

we obtain

$$x(t) = \frac{1}{\Omega_{ci}^2} \frac{|e| E}{m_i} + \frac{v_{y0}}{\Omega_{ci}} + x_0 - \frac{1}{\Omega_{ci}} \left(\frac{1}{\Omega_{ci}} \frac{|e| E}{m_i} + v_{y0} \right) \cos(\Omega_{ci} t) + \frac{v_{x0}}{\Omega_{ci}} \sin(\Omega_{ci} t) \quad (\text{C.11})$$

$$y(t) = y_0 - \frac{v_{x0}}{\Omega_{ci}} - \frac{1}{\Omega_{ci}} \frac{|e| E}{m_i} t + \frac{1}{\Omega_{ci}} \left(\frac{1}{\Omega_{ci}} \frac{|e| E}{m_i} + v_{y0} \right) \sin(\Omega_{ci} t) + \frac{v_{x0}}{\Omega_{ci}} \cos(\Omega_{ci} t) \quad (\text{C.12})$$

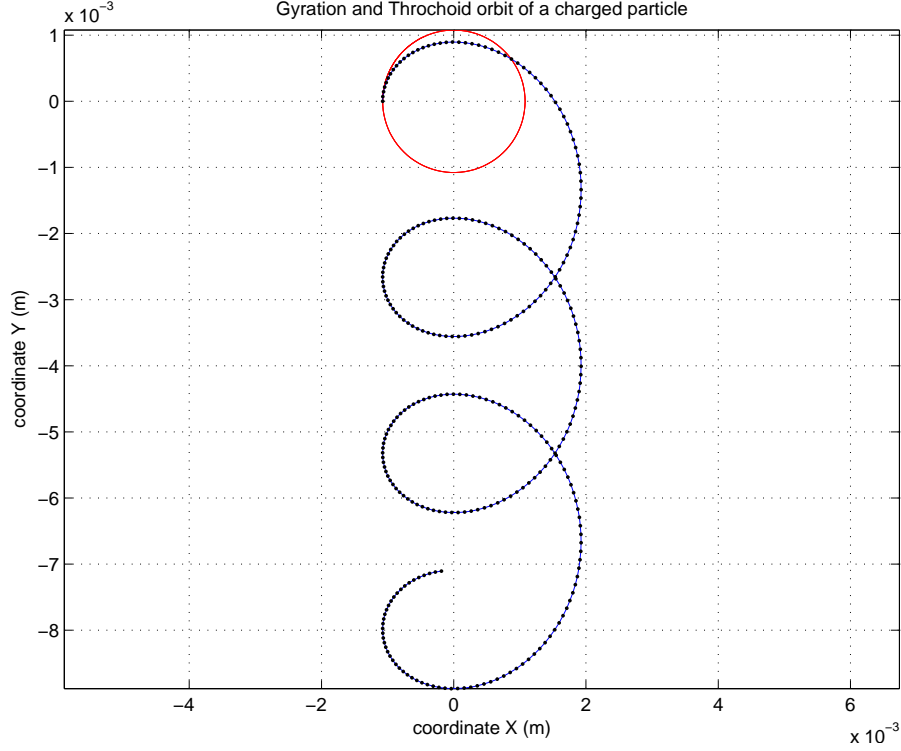


Figure 33: The deformation of the pure gyration orbit (red) into a trochoid (blue) under the effect of an electric field. A very high value of the electric field (350 kV/m) was used in order to make more visible the deformation. The plasma center is at right.

This curve (see Figure 33) is a *prolate trochoid*. The electric $E \times B$ motion is along the negative y axis. We adopt initial conditions ($x_0 = -\rho_i$, $y_0 = 0$, $v_{x0} = 0$, $v_{y0} = v_{th,i}$) that are identical for the static $E \neq 0$ as well as for pure gyration ($E \equiv 0$). In this way we can see how the *trochoid* is different of the Larmor circle. The orbit has, broadly, two unequal lobes. This asymmetry makes that the “center” of the positions of the particle to be shifted relative to the one of the pure Larmor gyration. For ions the shift is in the direction of the electric field \mathbf{E}^I . The ions are now more frequently present to the left of the symmetry axis of the previously symmetric (circle) orbit. There is an effective concentration of ions at the end of the interval on r to which points the electric field produced by the “external” \mathbf{E}^I (generated by ionization). For electrons there is a shift to the opposite direction but much smaller and will be neglected.

Therefore for a given \mathbf{E}^I there is an excess of ion charge at the left ($\sim r_1$) end of the ionization domain. A new layer (called L) of positive charge is generated at the left end, opposite to the ionization-induced layer I . The width δx^L is the amount of deformation

relative to the pure Larmor gyration orbit, *i.e.* the distance between the center of the *prolate trochoid* and the center of the Larmor circle, when both trajectories start from the same initial conditions, but with $E \neq 0$ respectively $E = 0$. To find it, we calculate the time evolution of the averages

$$\bar{x}(t) = \frac{1}{t} \int_0^t x(t') dt' \quad , \quad \bar{y}(t) = \frac{1}{t} \int_0^t y(t') dt' \quad (\text{C.13})$$

For large t

$$\bar{x}(t \rightarrow \infty) = \frac{1}{\Omega_{ci}^2} \frac{|e| E}{m_i} + \frac{v_{y0}}{\Omega_{ci}} + x_0 = \frac{1}{\Omega_{ci} B} E \quad (\text{C.14})$$

and

$$\bar{y}(t \rightarrow \infty) = y_0 - \frac{v_{x0}}{\Omega_{ci}} + \frac{1}{2} \left(-\frac{1}{\Omega_{ci}} \frac{|e| E}{m_i} \right) t = -\frac{E}{2B} t \quad (\text{C.15})$$

The *center* of the new orbit has a shift $\delta x^L = \bar{x}(t \rightarrow \infty) = \frac{1}{\Omega_{ci} B} E$. The electric field that occurs in the above equation is the *internal* field E^{int} , *i.e.* the ionization-induced field E^I from which we subtract the field generated by the new layer L , $E^{int} = E^I - E^L$. Using the shift $\delta x^L = \frac{1}{\Omega_{ci} B} E^{int}$ the surface charge density in the layer L is

$$\sigma^L = |e| n^{bg} \frac{1}{\Omega_{ci} B} E^{int} \quad \left(\frac{C}{m^2} \right) \quad (\text{C.16})$$

The electric field produced by the deformation of the Larmor gyration is

$$E^L = \frac{\sigma^L}{\varepsilon_0} = \frac{1}{\varepsilon_0} |e| n^{bg} \frac{1}{\Omega_{ci} B} E^{int} = \frac{c^2}{v_A^2} E^{int} \quad (\text{C.17})$$

from where we find $E^{int} = E^I - E^L = E^I - \frac{c^2}{v_A^2} E^{int}$, or

$$E^{int} = \frac{E^I}{1 + c^2/v_A^2} \quad (\text{C.18})$$

If the “external”, ionization-induced, electric field E^I continues to increase, there is *increase* in time of the deformation of the trochoid

$$\frac{d}{dt} \bar{x}(t \rightarrow \infty) = \frac{1}{\Omega_{ci} B} \frac{dE^{int}}{dt} \quad (\text{C.19})$$

which is precisely the *polarization drift* of the ions

$$v_{Di}^{(pol)} = \frac{1}{\Omega_{ci} B} \frac{dE^{int}}{dt} \quad (\text{C.20})$$

i.e. the drift of polarization simply consists of the time variation of the deformation $v_{Di}^{(pol)} = \frac{d}{dt} \bar{x}(t \rightarrow \infty)$.

The velocity of the polarization drift of the background ions (of density n^{bg})

$$v_{Di}^{(pol)} = \frac{1}{\Omega_{ci} B} \frac{1}{1 + c^2/v_A^2} \frac{dE^I}{dt} \approx \frac{\varepsilon_0}{|e| n^{bg}} \frac{dE^I}{dt} \quad (C.21)$$

is in general much smaller than the first order drift v_E and than the neoclassical drift v_{Di} . The estimated magnitude varies between $v_{Di}^{(pol)} \sim 0.02...10$ (m/s) according to \dot{n}_{ioniz} is determined by slow gas input or pellets. We would be tempted to expect a slower response of the background ions. The build-up of the charge layer induced by ionization is $\delta t = \Delta^t/v_{Di}$ while the build up of the charge layer induced by polarization drift is $\delta t^{(pol)} = \delta x^L/v_{Di}^{(pol)}$. However these two time scales are identical. Using Eqs.(C.19-C.20) and (C.18)

$$\delta t^{(pol)} = \frac{\delta x^L}{v_{Di}^{(pol)}} = \left(\frac{d}{dt} \ln E^I \right)^{-1} \quad (C.22)$$

and inserting Eq.(C.8) and $\delta t = \Delta^t/v_{Di}$ we find

$$\delta t^{(pol)} = \delta t \quad (C.23)$$

Using again Eq.(C.8) we obtain

$$v_{Di}^{(pol)} = \frac{1}{\Omega_{ci} B} \frac{1}{1 + c^2/v_A^2} \Delta^t \frac{1}{\varepsilon_0} |e| \dot{n}_{ioniz} = \Delta^t \frac{\dot{n}_{ioniz}}{n^{bg}} \quad (C.24)$$

This can be translated in the language of currents. By definition

$$J^{(pol)} = |e| n^{bg} v_{Di}^{(pol)} \quad (C.25)$$

and

$$J^I = |e| \Delta^t \dot{n}_{ioniz} \quad (C.26)$$

and Eq.(C.24) shows that the polarization current $J^{(pol)}$ is equal and opposite to the “externally” imposed current J^I .

$$J^I = J^{(pol)} \quad (C.27)$$

The plasma response $J^{(pol)}$ is the return current, involving the background ions.

REFERENCES

- ¹L. R. Baylor, T. C. Jernigan, S. K. Combs, W. A. Houlberg, M. Murakami, P. Gohil, K. H. Burrell, C. M. Greenfield, R. J. Groebner, C.-L. Hsieh, R. J. La Haye, P. B. Parks, G. M. Staebler, DIII-D Team, G. L. Schmidt, D. R. Ernst, E. J. Synakowski, and M. Porkolab. Improved core fueling with high field side pellet injection in the diiii-d tokamak. *Phys. Plasmas*, 7:1878–1885, 2000.
- ²L.R. Baylor, T.C. Jernigan, P.B. Parks, G. Antar, N.H. Brooks, S.K. Combs, D.T. Fehling, C.R. Foust, W.A. Houlberg, and G.L. Schmidt. Comparison of deuterium pellet injection from different locations on the diiii-d tokamak. *Nuclear Fusion*, 47(11):1598, 2007.
- ³L.R. Baylor, G.L. Schmidt, W.A. Houlberg, S.L. Milora, C.W. Gowers, W.P. Bailey, M. Gadeberg, P. Kupschus, J.A. Tagle, D.K. Owens, D.K. Mansfield, and H.K. Park. Pellet fuelling deposition measurements on jet and tftr. *Nuclear Fusion*, 32(12):2177, 1992.
- ⁴R E Bell, F M Levinton, S H Batha, E J Synakowski, and M C Zarnstorff. Core poloidal rotation and internal transport barrier formation in tftr. *Plasma Physics and Controlled Fusion*, 40(5):609, 1998.
- ⁵H.A. Berk and A.A. Galeev. Velocity space instabilities in a toroidal geometry. *Phys. Fluids*, 10:441–450, 1967.
- ⁶C. L. Fiore, D. R. Ernst, J. E. Rice, K. Zhurovich, N. Basse, P. T. Bonoli, M. J. Greenwald, E. S. Marmor, and S. J. Wukitch. Internal transport barriers in alcator c-mod. *Fusion Science and Technology*, 51:303–316, 2007.
- ⁷B.H. Fong and T.S. Hahm. Bounce averaged kinetic equations and neoclassical polarization density. *Physics of Plasmas*, 6:189–199, 1999.
- ⁸T. Fulop, Peter J. Catto, and P. Helander. Neutral diffusion and anomalous effects on collisional ion flow shear in tokamaks. *Physics of Plasmas (1994-present)*, 5(11):3969–3973, 1998.
- ⁹A.A. Galeev and R.Z. Sagdeev. Theory of neoclassical diffusion. In M.A. Leontovich, editor, *Reviews of Plasma Physics*, volume 7, pages 257–343. Consultants Bureau, New York, 1979.
- ¹⁰Adil B. Hassam and Russell M. Kulsrud. Time evolution of mass flows in a collisional tokamak. *Physics of Fluids (1958-1988)*, 21(12):2271–2279, 1978.

- ¹¹F.L. Hinton and R.D. Hazeltine. Theory of plasma transport in toroidal confinement systems. *Rev. Mod. Phys.*, 48:239–308, 1976.
- ¹²F.L. Hinton and M.N. Rosenbluth. The mechanism for the toroidal momentum input to tokamak plasma from neutral beams. *Phys. Letters*, A259:267–275, 1999.
- ¹³W.A. Houlberg, S.E. Attenberger, L.R. Baylor, M. Gadeberg, T.C. Jernigan, P. Kuschus, S.L. Milora, G.L. Schmidt, D.W. Swain, and M.L. Watkins. Pellet penetration experiments on jet. *Nucl. Fusion*, 32:1951–1965, 1992.
- ¹⁴M. Hugon, B.Ph. van Milligen, P. Smeulders, L.C. Appel, D.V. Bartlett, D. Boucher, A.W. Edwards, L.-G. Eriksson, C.W. Gowers, T.C. Hender, G. Huysmans, J.J. Jacquinot, P. Kupschus, L. Porte, P.H. Rebut, D.F.H. Start, F. Tibone, B.J.D. Tubbing, M.L. Watkins, and W. Zwingmann. Shear reversal and mhd activity during pellet enhanced performance pulses in jet. *Nuclear Fusion*, 32(1):33, 1992.
- ¹⁵G.L. Jackson, M. Murakami, G.R. McKee, D.R. Baker, J.A. Boedo, R.J. La Haye, C.J. Lasnier, A.W. Leonard, A.M. Messiaen, J. Ongena, G.M. Staebler, B. Unterberg, M.R. Wade, J.G. Watkins, and W.P. West. Effects of impurity seeding in diii-d radiating mantle discharges. *Nuclear Fusion*, 42(1):28, 2002.
- ¹⁶P T Lang, B Alper, L R Baylor, M Beurskens, J G Cordey, R Dux, R Felton, L Garzotti, G Haas, L D Horton, S Jachmich, T T C Jones, A Lorenz, P J Lomas, M Maraschek, H W Mller, J Ongena, J Rapp, K F Renk, M Reich, R Sartori, G Schmidt, M Stamp, W Sut-trop, E Villedieu, D Wilson, and EFDA-JET workprogramme collaborators. High density operation at jet by pellet refuelling. *Plasma Physics and Controlled Fusion*, 44(9):1919, 2002.
- ¹⁷Wandong Liu and M. Talvard. Rapid global response of the electron temperature during pellet injection on tore supra. *Nuclear Fusion*, 34(3):337, 1994.
- ¹⁸A.I. Morozov and L.S. Solovév. Motion of charged particles in electro-magnetic fields. In M.A. Leontovich, editor, *Reviews of Plasma Physics*, volume 2, pages 201–297. Consultants Bureau, New York, 1966.
- ¹⁹J. Nycander and V.V. Yankov. H-mode in tokamaks attributed to absence of trapped ions in poloidally rotating plasma. *Pisma Zh. Eksp. Teor. Fiz.*, 63(6):427–430, 1996.
- ²⁰J. E. Rice, W. D. Lee, E. S. Marmor, N. P. Basse, P. T. Bonoli, M. J. Greenwald, A. E. Hubbard, J. W. Hughes, I. H. Hutchinson, A. Ince-Cushman, J. H. Irby, Y. Lin, D. Mosses-sian, J. A. Snipes, S. M. Wolfe, S. J. Wukitch, and K. Zhurovich. Toroidal rotation and

- momentum transport in alcator c-mod plasmas with no momentum input. *Physics of Plasmas (1994-present)*, 11(5):2427–2432, 2004.
- ²¹J.E. Rice, B.P. Duval, M.L. Reinke, Y.A. Podpaly, A. Bortolon, R.M. Churchill, I. Cziegler, P.H. Diamond, A. Dominguez, P.C. Ennever, C.L. Fiore, R.S. Granetz, M.J. Greenwald, A.E. Hubbard, J.W. Hughes, J.H. Irby, Y. Ma, E.S. Marmor, R.M. McDermott, M. Porkolab, N. Tsujii, and S.M. Wolfe. Observations of core toroidal rotation reversals in alcator c-mod ohmic l-mode plasmas. *Nuclear Fusion*, 51(8):083005, 2011.
- ²²M. N. Rosenbluth, R. D. Hazeltine, and F. L. Hinton. Plasma transport in toroidal confinement systems. *Physics of Fluids (1958-1988)*, 15(1):116–140, 1972.
- ²³M.N. Rosenbluth and F.L. Hinton. Plasma rotation driven by alpha particles in a tokamak reactor. *Nucl. Fusion*, 36:55–67, 1996.
- ²⁴P. Smeulders, L.C. Appel, B. Balet, T.C. Hender, L. Lauro-Taroni, D. Stork, B. Wolle, S. Ali-Arshad, B. Alper, H.J. De Blank, M. Bures, B. De Esch, R. Giannella, R. Konig, P. Kupschus, K. Lawson, F.B. Marcus, M. Mattioli, H.W. Morsi, D.P. O’Brien, J. O’Rourke, G.J. Sadler, G.L. Schmidt, P.M. Stubberfield, and W. Zwingmann. Survey of pellet enhanced performance in jet discharges. *Nuclear Fusion*, 35(2):225, 1995.
- ²⁵F. Spineanu and M. Vlad. Fluctuation of the ambipolar equilibrium in magnetic perturbations. *Physics of Plasmas*, 9(12):5125–5128, 2002.
- ²⁶F. Spineanu and M. Vlad. A model for the reversal of the toroidal rotation in tokamak. *Nuclear Fusion*, 52:114019, 2012.
- ²⁷F. Spineanu and M. Vlad. The role of the rotation in the correlated transient change of the density and confinement. 40th EPS Conference on Plasma Physics, 2013. Helsinki, Finland, 1-5 July 2013. Paper P1.178.
- ²⁸Julius Adams Stratton. *Electromagnetic Theory*. McGraw-Hill Book Company, 1941.
- ²⁹M.R. Tournianski, P.G. Carolan, N.J. Conway, G.F. Counsell, A.R. Field, and M.J. Walsh. Poloidal rotation and associated edge behaviour in start plasmas. *Nuclear Fusion*, 41(1):77, 2001.
- ³⁰M. Valovic, L. Garzotti, C. Gurl, R. Akers, J. Harrison, C. Michael, G. Naylor, R. Scannell, and the MAST team. H-mode access by pellet fuelling in the mast tokamak. *Nuclear Fusion*, 52(11):114022, 2012.
- ³¹S.K. Wong and K.H. Burrell. Transport theory of tokamak plasmas with large toroidal rotation. *Phys. Fluids*, 25:1863–1870, 1982.